UNCLASSIFIED

ENCE COPY

O

008

BRL

REPORT NO. 1084

NOVEMBER 1959

EFFECTS OF ANISOTROPIES IN ROTARY
EXTRUDED LINERS (U)

FOR REFERENCE

C. M. GLASS

M. K. GAINER

G. L. MOSS

COUNTED IN

NOT TO BE TAKEN FROM THE ROOM

BD 23 012

TECHN...
B...
ABERDEEN PROVING GROUND, MD
STEAP-TL

BALLISTIC RESEARCH LABORATORIES

ABERDEEN PROVING GROUND, MARYLAND

UNCLASSIFIED

APR 1970

Retain or destroy per AR 380-5 and AR 345-220, or comparable Navy or AF Regulations. Contractors should consult their government contracting offices regarding procedures to be followed. DO NOT RETURN
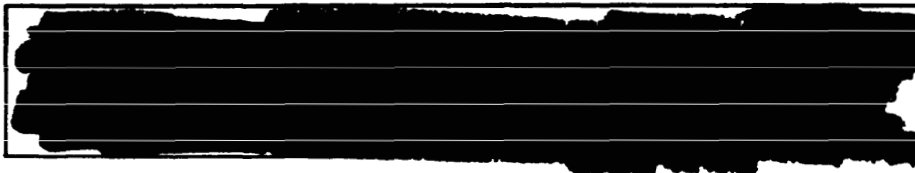
BALLISTIC RESEARCH LABORATORY

REPORT NO. 1084

NOVEMBER 1959

EFFECTS OF ANISOTROPIES IN ROTARY EXTRUDED LINERS (U)

C. M. Glass
M. K. Gainer
G. L. Moss

ABERDEEN PROVING GROUND, MARYLAND

TABLE OF CONTENTS

BALLISTIC RESEARCH LABORA██████████

REPORT NO. 1084

EFFECTS OF ANISOTROPIES IN ROTARY EXTRUDED LINERS (U)

██████████   ABSTRACT

Conical shaped charge liners manufactured by the rotary extrusion process exhibit a characteristic "spin compensation" not found in an ordinary liner. It has been determined that this ability to counteract degradation of the jet when the round is being subjected to an external rotation is dependent on the manner in which certain crystal planes are aligned with respect to the surface of the cone. Direct correlation between the preferred orientation of the planes and the spin compensation frequency has been found. In addition, it has been demonstrated that other factors, such as residual stress, grain shape, etc., do not influence the compensation rate.

It is proposed that under detonation loading there exists a component of collapse velocity of the liner wall that is not directed toward the axis of the cone. This tangential component results from the preferred orientation of the crystal planes, and gives an angular velocity to the collapsing cone elements that compensates for the angular velocity due to external rotation of the round. Experimental evidence is offered to show that a metal having a strong preferred orientation will deform anisotropically under detonation loading.

LIST OF TABLES

C

C

C

C

C

C

UNCLASSIFIED

ACKNOWLEDGEMENTS

I. INTRODUCTION

This paper reports the results of an investigation into metal-lurgical or "built-in" spin compensation in conical shaped charge liners, and offers an explanation for the existence of this phenomenon. Spin compensation is the ability of a shaped charge to compensate for an external rotation applied to it, thus allowing the jet formed by the liner to be normal and unaffected by the external rotation. This implies that, during collapse, the liner elements are given a rotation equal and opposite in magnitude to the rotation applied to the system.

The theory of shaped charge operation was formulated by Pugh and coworkers,[1,2*] and extended by the systematic analysis of Eichelberger[3,4]. The pressures experienced by the conical shaped charge liner, during the explosive detonation, were considered high enough to cause the metal to react as a fluid, and hydrodynamic theory was applied. The liner collapses toward its axis, where part of the metal goes forward rapidly as a jet, and the remaining metal forms a slower moving slug.

Figure 1 shows a cross section of a shaped charge round. General use has been with fin-stabilized rounds, but many requirements exist for spin-stabilized projectiles having rotational frequencies ranging from 45 rps to approximately 2000 rps. Under rotation, the jet from a normal shaped charge liner bifurcates, or breaks up into parallel ribbons of material, as seen in Figure 2. Figure 3 is a curve showing the penetration depth of a normal liner vs. the frequency of rotation of the round. The decrease in penetration is directly related to the bifurcation of the jet.

The problem of obtaining a liner that will provide spin compensation has been recognized for a number of years, and numerous schemes have been tried to produce a spin-compensating round. The most successful approach to date has been the use of liners with fluted inner and outer walls,[5,6] and is currently under development by Eichelberger and coworkers.

---

* Numbers above the line refer to the bibliography at the end of the paper.

9

FIG. I — CROSS SECTION OF A SHAPED CHARGE ROUND

(a)   (b)   (c)   (d)   (e)
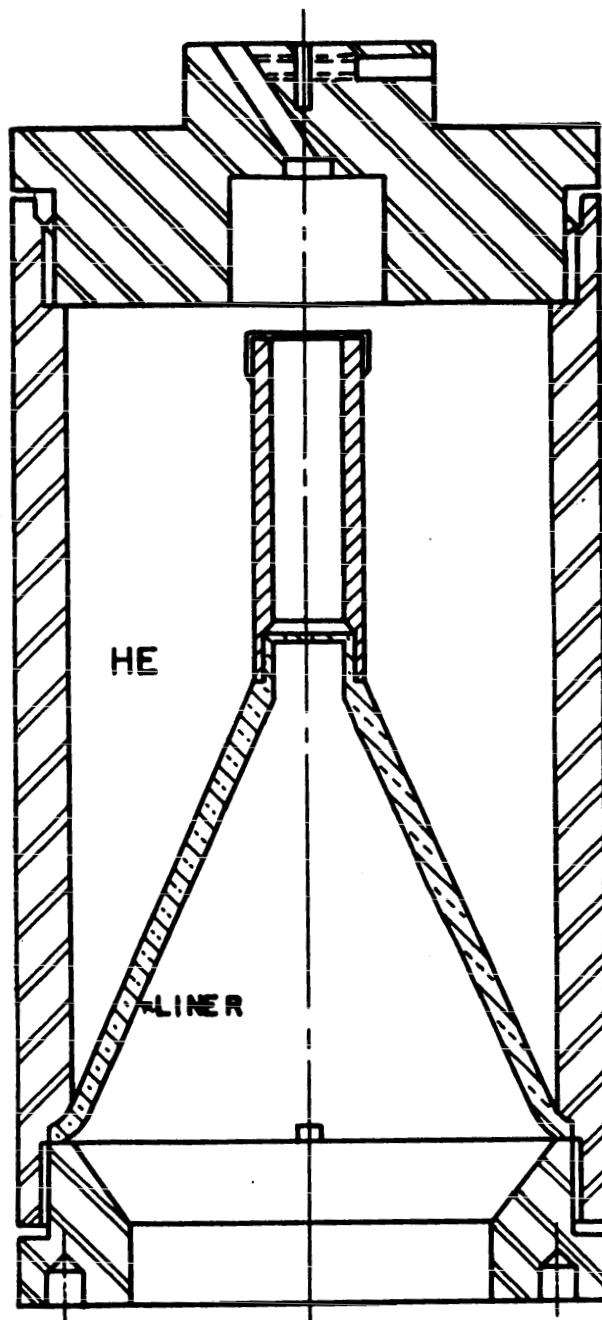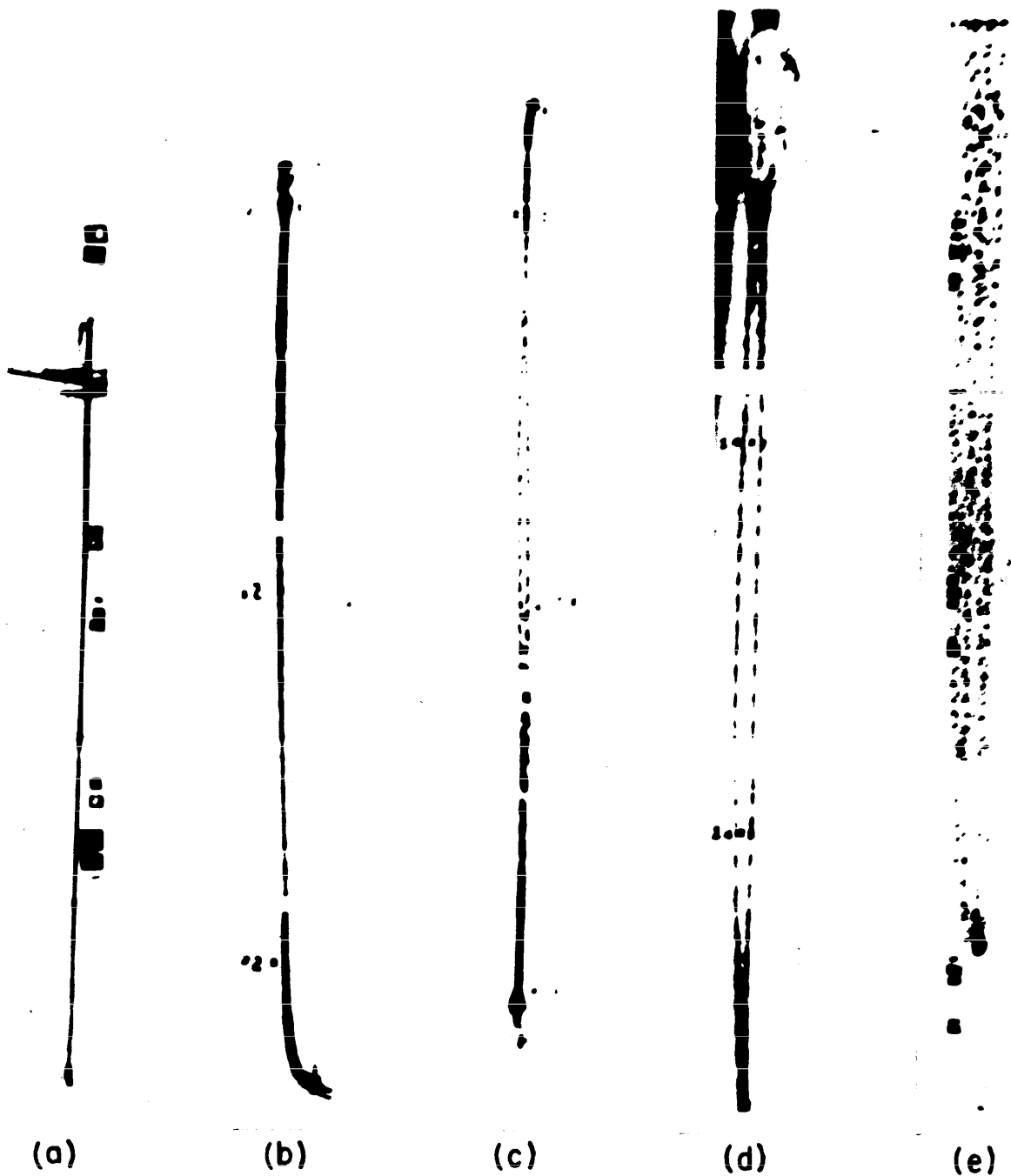
THE JET OF A SMOOTH 105 MM LINER IS SHOWN TO
SPREAD WHEN THE SHAPED CHARGE IS ROTATED. ROTATIONAL
FREQUENCIES FOR THESE JETS ARE (a) 0 RPS, (b) 15 RPS,
(c) 30 RPS, (d) 45 RPS, AND (e) 90.

FIGURE 2
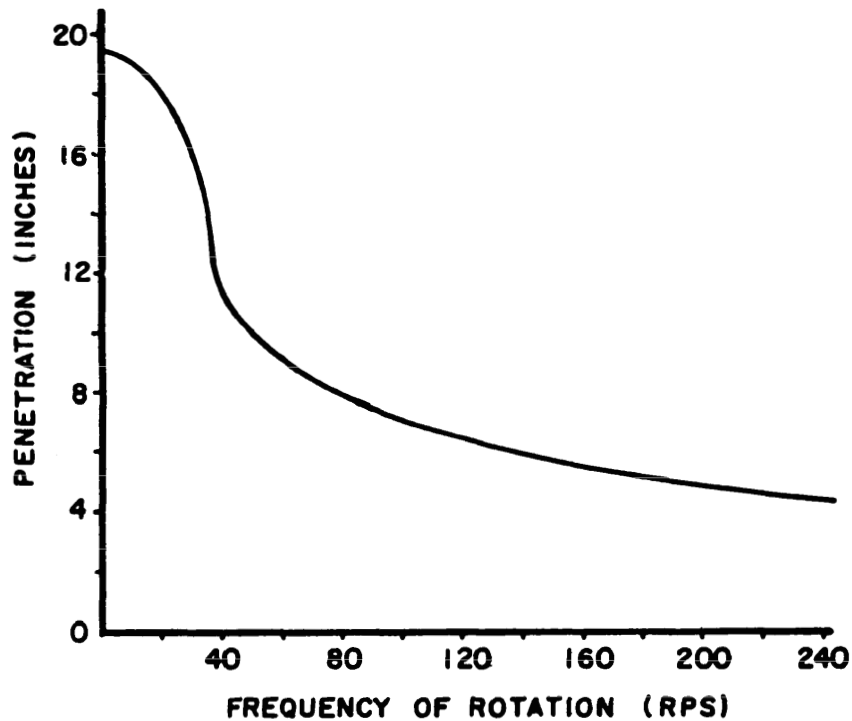
FIG. 3 — EFFECT OF ROTATION ON PENETRATION
FOR 105 MM Cu LINER

A method used to achieve limited spin-compensating frequencies that does not depend on geometrical changes of the liner was discovered during the investigation of a manufacturing technique for shaped-charge cones. The process is known as the "rotary-extrusion" or "shear-forming" process, and is a mechanical modification of the standard metal-spinning technique. A round blank of metal, slightly cupped in the center, is held firmly against a rotating mandrel (see Figure 4). A circular, friction-driven, Carboloy tool moves in against the metal blank and travels down the side of the mandrel, maintaining a preset distance between the mandrel and the tool edge. The pressure exerted by the tool forces the metal blank to assume the conical shape of the mandrel and a thickness equal to the preset distance. Once the cone is formed, the excess blank material is removed from the cone base. Critical factors in the process are: the shape of the tool edge; the velocity of mandrel rotation; the velocity at which the tool travels down the mandrel; the blank hardness; the direction of rotation of the mandrel; and the temperature of the finished cone.

The fact that jets from cones manufactured by this process bifurcated when fired statically, indicated the possibility that spin compensation was present in the liner. Work by Winn[7] showed a spin-compensating frequency of 45 rps, taken from the penetration-rotation curve reproduced in Figure 5. This frequency is too low for most applications, but could be useful for special slow-spin rounds. Studies were begun to determine the cause of this "built-in" spin compensation.

13

A ROTATION AROUND THE APEX
TO ACCOMMODATE DIFFERENT
CONE ANGLES.

LIVE CENTER

TOOL

CUPPED DISK ON MANDREL

MANDREL
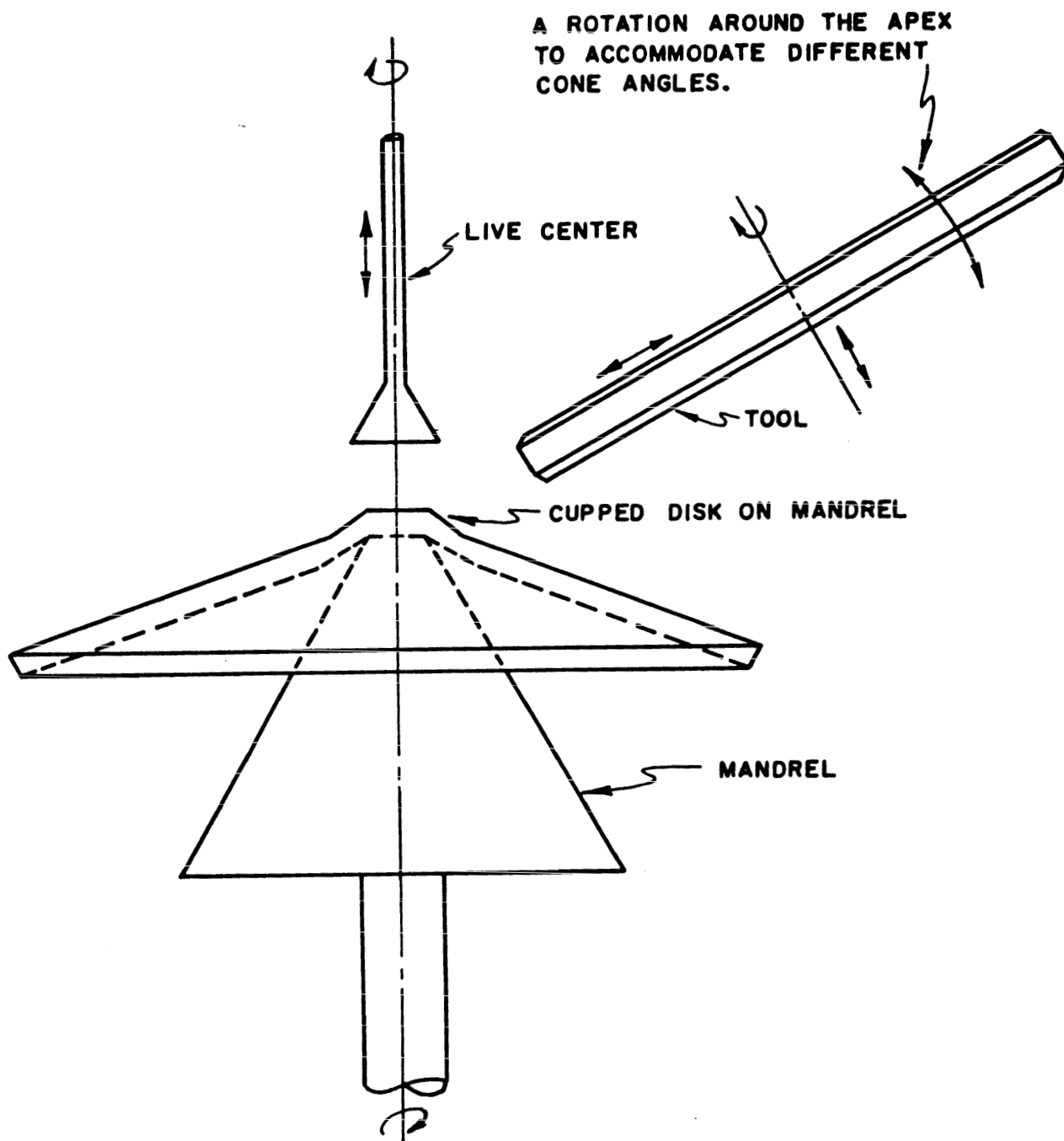
FIG. 4 — SCHEMATIC DIAGRAM OF THE ROTARY
EXTRUSION PROCESS.
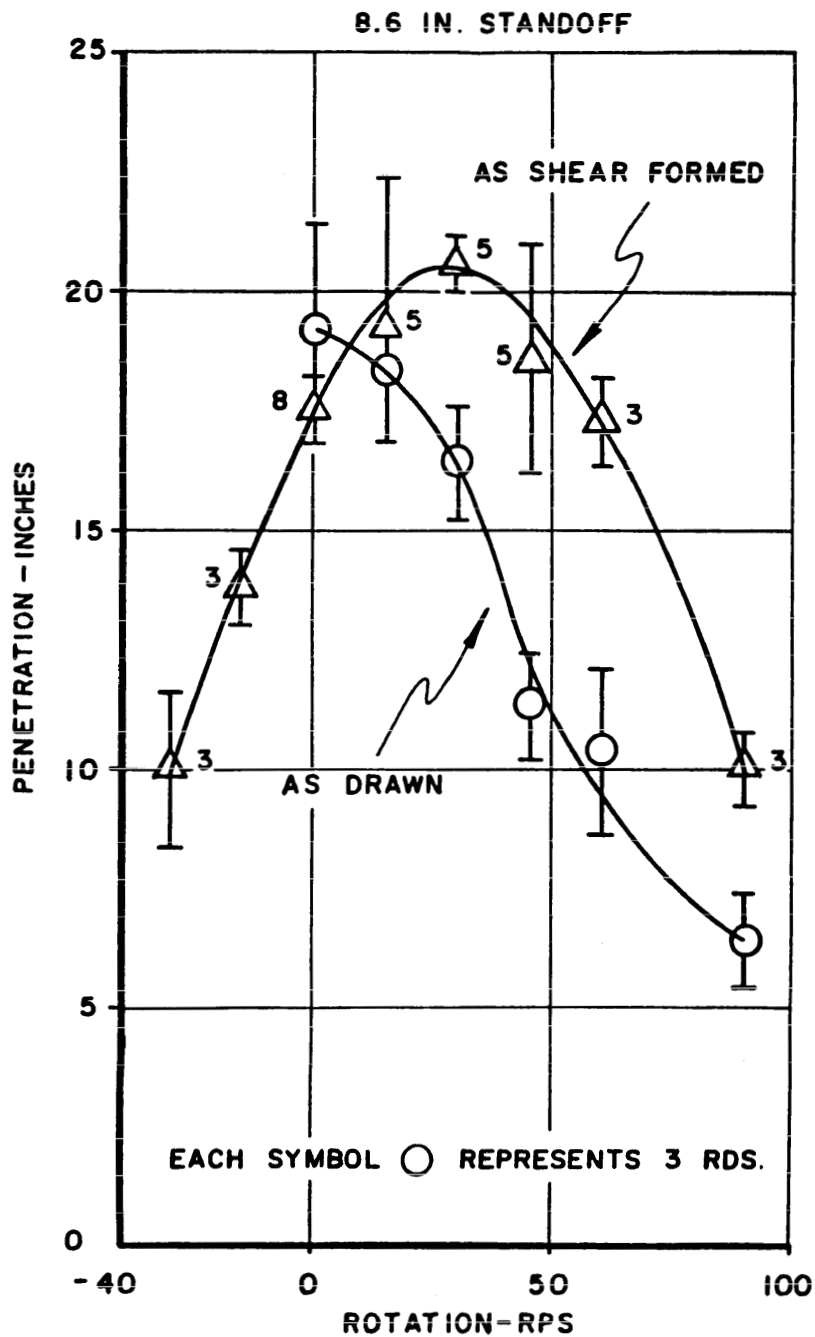
FIG. 5 – ROTATION-PENETRATION CURVE FOR
A ROTARY EXTRUDED LINER.
(FROM FIRESTONE TIRE AND RUBBER CO.)

■■■■■■■ II. PREVIOUS INVESTIGATIONS

A. Methods of Observing Spin Compensation

The two principal means of observing spin compensation in a shaped charge are:

1. Penetration-rotation studies.

2. Flash X-Ray studies of the jet at different rotation frequencies.

The first method is rather laborious, since a number of rounds must be fired into targets at each frequency of rotation to determine the optimum compensation frequency for the point of maximum penetration. The second method consists of detonating rotating rounds and taking flash radiographs of the jets.[8] Simon and coworkers used three flash X-Ray units to photograph the jet at different times, and showed (by comparing their results with penetration-rotation curves) that the spin compensation frequency may be taken as the frequency at which the jet is the least bifurcated.[9, 10, 11]

B. Results of Previous Investigations

The spin-compensation frequency of a rotary-extruded liner varies with the speed of the tool down the mandrel. Present data indicates that the variation is not linear and that the same speed on blanks rotated clockwise and counterclockwise produces spin frequencies of opposite sign but not of equal magnitude.[13] A number of experiments have been performed in the past to determine the mechanism causing this spin compensation. Following is a brief list of the more significant results obtained:

1. An empirical relationship exists between the "angle of twist" given to scribe lines placed on the blank before forming, and the compensation frequency.[12]

2. Manufacturing parameters affect to a great extent the optimum spin compensation frequency but not the penetration at optimum frequency.[13]

16

3. Annealing a rotary-extruded cone above its recrystalization temperature destroys the spin compensation.[14]

4. Electroformed liners spin compensate at frequencies as high as 40 rps when the mandrel on which the cones are formed is not rotated during forming. Rotation of the mandrel during the electro-forming operation eliminates the spin compensation.[15, 16]

5. Metals other than copper also show compensation when rotary extruded. For instance: Armco Iron shows a compensation frequency of 60 rps under certain manufacturing conditions; brasses compensate, as do nickel liners. Lead-antimony does not show any compensation when rotary extruded.[12, 17, 18, 19]

6. Rotary-extruded liners have a strongly preferred grain orientation. In single-crystal aluminum liners when the $\langle 100 \rangle$ direction lies along the liner axis the results are the same as for normal liners, but when the $\langle 110 \rangle$ direction lies along the liner axis, the jet bifurcates.[20, 21, 22]

7. Liners machined from cylindrical bars of copper and given a torsional twist around the cylinder axis show no compensation.[23]

C. Theoretical Considerations

A simplified representation of the effect of rotation on the shaped charge is seen in Figure 6, a and b. One element in a cross-sectional ring from a conical liner is considered. This element will have a collapse velocity of V_o directed toward the cone axis (Figure 6a). If an external rotation of ω is imposed on the cone, each element in a circular ring will be directed off the cone axis by an amount

$$r' = \frac{\omega r_o^2}{V_o \, \text{Cos} \, (\frac{\Theta + \beta}{2})} \quad ^*$$

(Figure 6b). If all elements perform similarly, the jet will rotate and separate or bifurcate as it moves toward the target. The compensation in a liner must therefore be equal and opposite to the external rotation to cancel this effect.

Several theories have been proposed concerning the cause of the built-in spin compensation in rotary-extruded liners. These theories are discussed in detail in the specific sections dealing with investigations concerning them, but a brief outline of them is presented here.

1. <u>Residual Stress Effect</u>. If a residual stress exists in the cone, arising from the manufacturing process, and if this stress is properly oriented with respect to the cone axis a greater resistance to collapse is offered by the stress in one direction. A slight torque is produced in the liner element which can then compensate for the rotation imposed externally.

---

* In deriving this equation, the relationship $\dfrac{\omega r_o}{r} = \dfrac{V_o \, \text{Cos} \, (\Theta + \beta)}{r_o}$ is used, and it is assumed that $r' \cong r$ when $\omega r_o \ll V_o \, \text{Cos} \, (\frac{\Theta + \beta}{2})$. (See, for instance, the Ordnance Corps Shaped Charge Reports, Volume 1, 1954, or Volume 1-56, 1956; and Critical Review of Shaped Charge Information, BRL Report No. 905, May, 1954).

COLLAPSE DIRECTION
AND VELOCITY OF
CONE ELEMENT

V_D DETONATION WAVE

ORIGINAL CONE WALL

NEW CONE
WALL DURING
COLLAPSE

V_0

β

θ

$\frac{1}{2}(\theta+\beta)$

(b)

CROSS SECTION OF CONE
DURING COLLAPSE

ωr_0

RESULTANT OF

$V_0 \cos \frac{(\theta+\beta)}{2}$ AND

ωr_0.

$V_0 \cos \frac{(\theta+\beta)}{2}$

r'

r

r_0

(a)
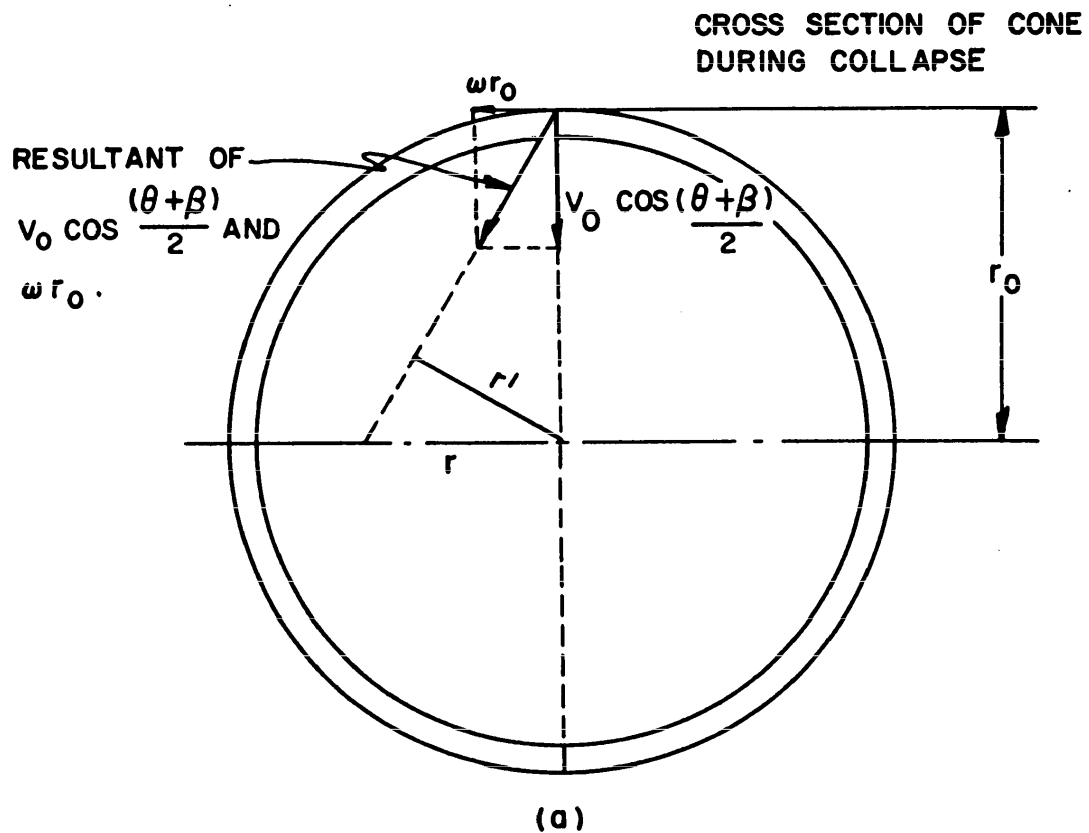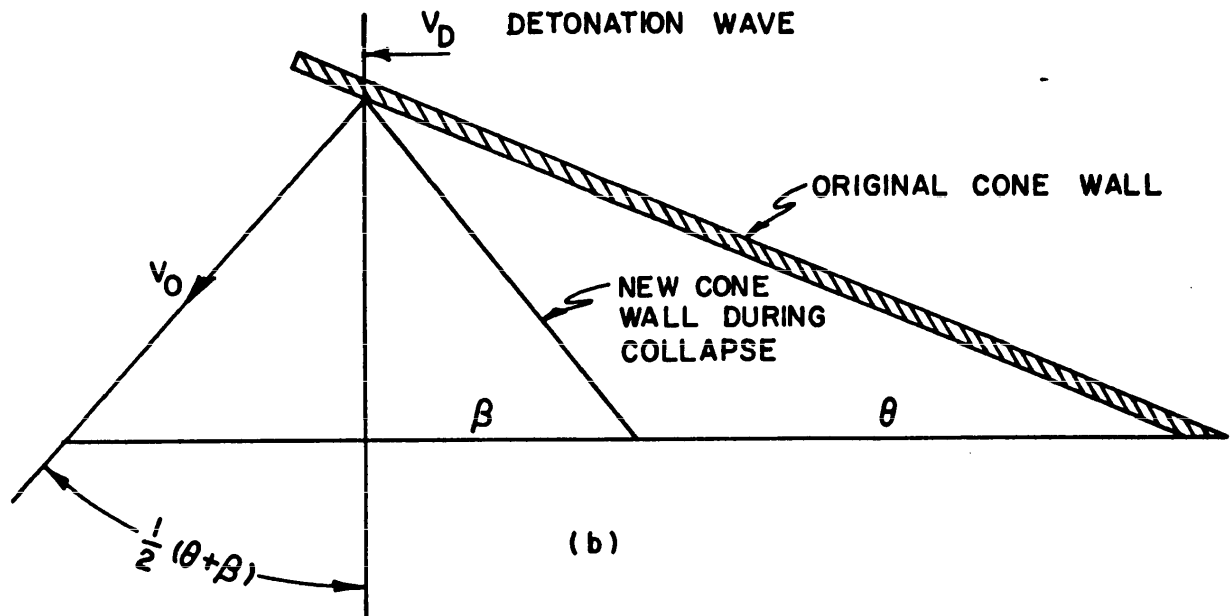
FIG. 6 — SCHEMATIC OF CONE COLLAPSE WITH ANGULAR VELOCITY

2. <u>Preferred Grain Shape and/or Impurity Distribution</u>. Under
the hydrodynamic theory of collapse, the metal flows without regard
to crystal structure. Since grain boundaries are harder than the
grains at room temperature, an arrangement of elongated grains may
be assumed whereby an "easy-flow" direction exists due to the grain
shape. If this easy collapse direction is properly oriented with
respect to the cone axis, the component of collapse directed off
the cone axis can provide compensation for a component of collapse
that arises from the external rotation.

Impurity distribution could lead to the same thing, because
of the increased hardness of the impurities compared with the base
metal. Combinations of grain shape and impurities would give rise to
the same effect.

3. <u>Preferred Orientation Effect</u>. Experiments on single crystals
indicate that different orientation of certain planes to the cone axis
give different effects on jet formation. Consequently the presence of
a preferred orientation of the crystal structure in the rotary-extruded
cones could give the same reaction as the single crystal; that is,
provide a path down certain planes where the deformation wave could
move more easily than in the rest of the metal. This would give a
preferred collapse direction and consequently give rise to spin compen-
sation.

4. <u>Combinations</u>. Combinations of any of the possible causes listed
above could produce the observed effect. Possibly none of the effects
listed are important, and some other mechanism should be considered.

A. Introduction

An investigation using eleven different lots of cones was conducted to determine the cause of spin compensation in rotary extruded liners. Each lot of cones had a different spin-compensation frequency, due to being formed with a different speed of movement of the tool down the mandrel. By rotating the mandrel, with the blank attached, clockwise or counterclockwise when viewed from the base, the spin compensation was made to occur in either a counterclockwise or clockwise direction (designated - or+respectively, in the rest of the report). The range of compensation frequencies in the eleven lots of liners was from -30 to +45 rps as determined by J. Simon.[13] Table I lists some of the parameters important to the spin compensation effect for the eleven lots of liners.

The blank material used in the manufacturing process was OFHC (oxygen-free, high conductivity) copper, 0.250" thick and 3" in diameter. The cone formed is shown in cross-section in Figure 7. It has a wall thickness of 0.090", an apex angle of 45° and an overall base diameter of 3.25". Figure 7 also illustrates the "angle of twist" mentioned previously. This was determined for each lot of liners by measuring the displacement at the base of the scribe lines marked on the blank.

The temperature of the cone after forming was in the neighborhood of $300^{\circ}F$, even though the cone is cooled during forming. Excess material was removed from the base of the finished product.

The experiments performed on this problem are reported in the following sections. The results of the investigations, together with tentative conclusions are reported in each section, and general conclusions are made under Section IV.

TABLE I

Manufacturing Parameters and Properties of Rotary Extruded Copper Liners Investigated

Cone Lot Letter	Mandrel Speed rpm	Tool Speed "/min	Angle of Twist(deg.)	Cone Temperature $^\circ$F	Mandrel Rotation Direction	Spin Compensation Frequency rps
A	1800	4.83	-15	300	clockwise	-25
B	1800	2.67	-10	290	clockwise	-20
C	1800	0.78	-4	265	clockwise	-8
D	1800	0.75	0	260	counterclockwise	+10
E	1800	1.13	+5.5	235	counterclockwise	+10
F	1800	1.78	+10	260	counterclockwise	+15
G	1800	2.49	+15	265	counterclockwise	+20
H	1800	3.74	+20	285	counterclockwise	+22
I	1800	5.67	+25	265	counterclockwise	+22
J	1800	11.70	+34	310	counterclockwise	+25
K	1800	17.02	+45	310	counterclockwise	+35
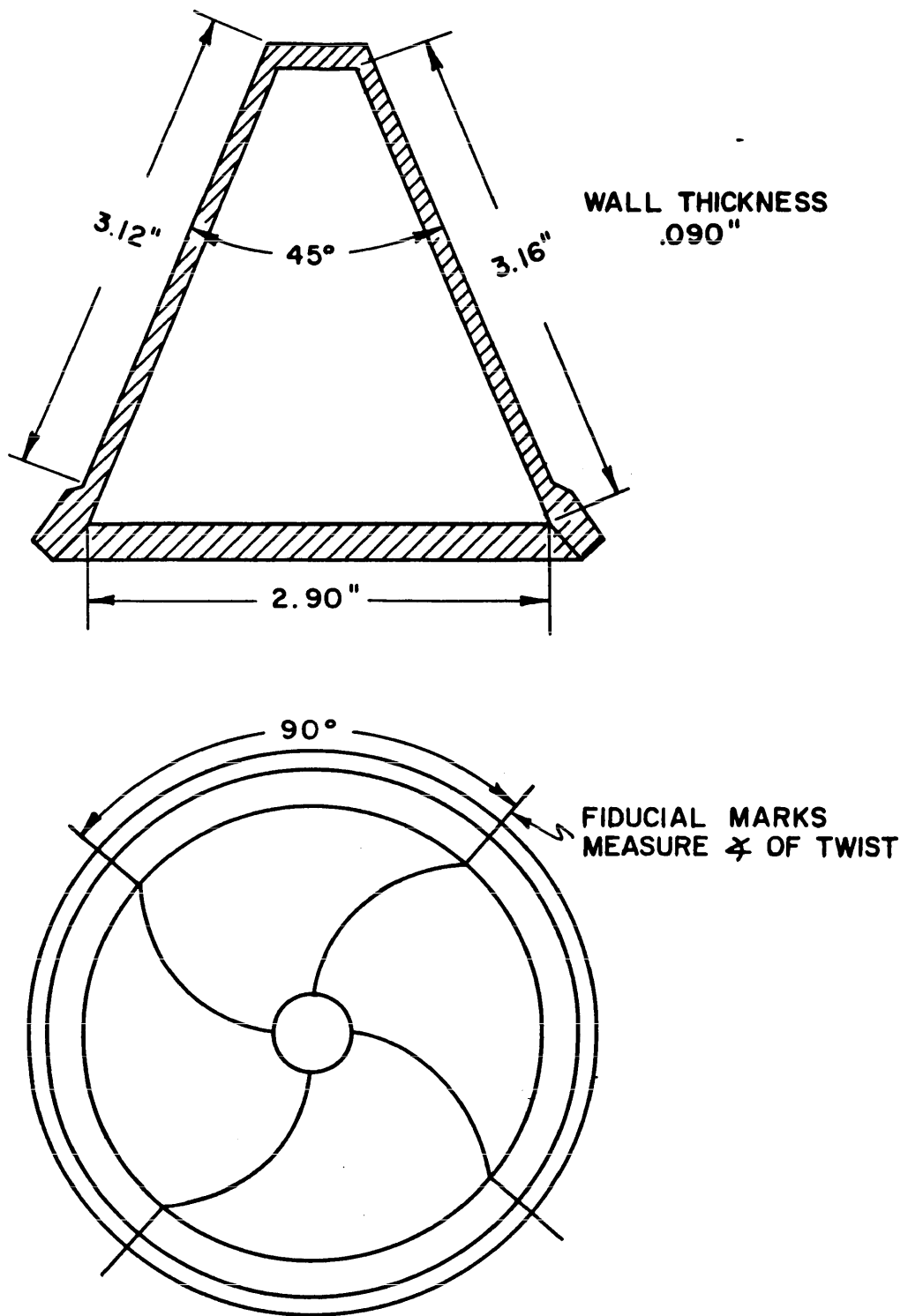
FIG. 7 — CONE DIMENSIONS OF THE CRAFT LINER SERIES

B. Residual Stress Studies

1. <u>Theoretical</u>. The rotary extrusion process undoubtedly leaves a residual stress in the cone. It should be noted, however, that surface temperatures of $300°F$ are measured even though the cone is being cooled during forming. Maximum temperatures in the cone are probably one to two hundred degrees higher. Under such temperature conditions, it would be unlikely that a large amount of residual stress would be present in the lattice.

Carrier and Prager[24] concluded that the stress necessary to produce any effect would have to be a residual shearing stress, and analyzed the effect of this type of stress on the performance of a collapsing ring taken from the cone as shown in Figure 8, a, b and c. The following symbols are used:

l = length of the section

a = radius of the section

δ = wall thickness

τ = residual stress in the wall, distributed as seen in Figure 8b

z = circular element axis

ρ = density of copper

Y = yield stress of copper

V = velocity of the shock wave in the metal

r = distance from the element being considered to the cylinder axis

It is assumed that:

(a) The residual shearing stresses are not destroyed by shear waves from another part of the cylinder, because the cylinder collapses under the influence of a detonation wave that travels with a velocity faster than the velocity of shear waves.
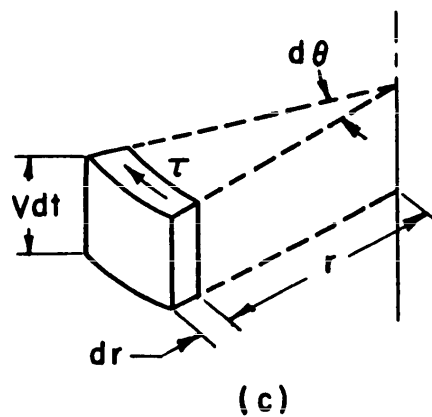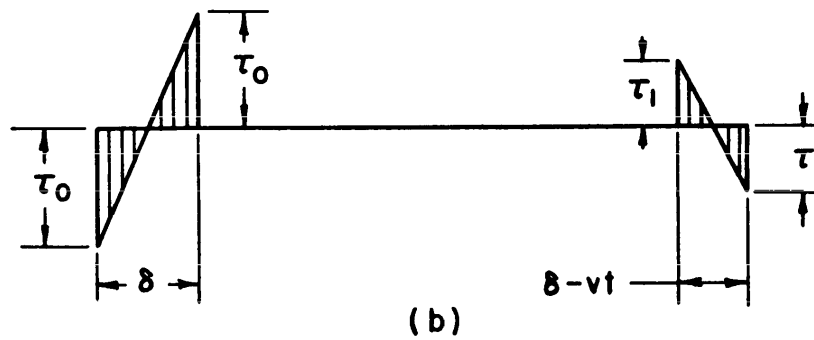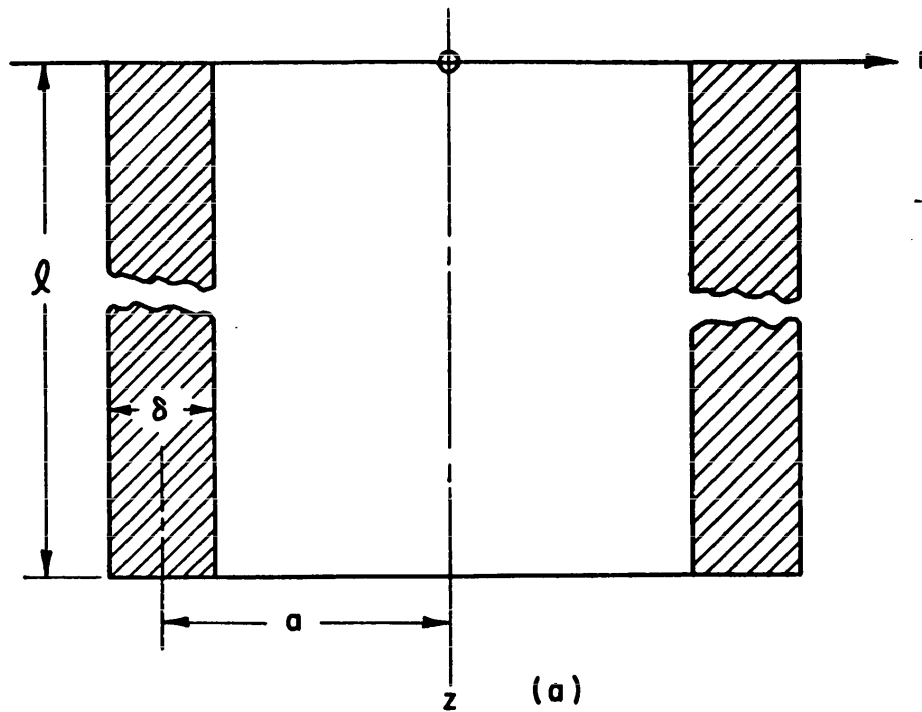
FIG. 8—SCHEMATIC FOR CALCULATING RESIDUAL
STRESS EFFECTS IN LINERS
(SEE REFERENCE 24 FOR
ADDITIONAL DETAILS)

(b) The shearing stress can make itself felt during the time necessary for collapse of the section.

The shearing stress, τ, will then give an angular velocity ω to the element. Since the jet comes from the inner wall of the cone and the slug from the rest of the wall, the jet and slug would be spinning in opposite directions because of the opposite orientation of shearing stresses shown in Figure 8. If Ω is the rotation velocity of the jet, the following equation is derived for the jet element a distance D from the jet axis*:

$$\Omega = \frac{Y\delta}{2\rho VD^2} = \frac{\tau_o\, a}{\rho V\, D^2} \qquad (1)$$

Applying the equation to a 105mm copper liner, Carrier and Prager concluded that the residual stresses that might be present in a copper cone could give a 20 rps spin compensation frequency.

The present authors have assumed that, if a shearing stress may be retained in the material of sufficient magnitude to cause the desired effect, a simple analysis will approximate the stress conditions in the material to at least as high a degree of accuracy as that expected from the assumptions of Carrier and Prager. Using two-dimensional elastic theory, a system of stress as seen in Figure 9 is described by a polynomial stress function of the fifth degree when certain substitutions are made (See, for instance, Timoshenko and Goodier, "Theory of Elasticity"). The following relations are developed by this simplified approach:

$$\sigma_x = d_5\, (x^2 y - 2/3 y^3) \qquad (2)$$

$$\sigma_y = 1/3\, d_5 y^3 \qquad (3)$$

$$\tau_{xy} = -d_5 x y^2 \qquad (4)$$

---

*   For a complete description of this analysis, see Reference 24.

where: σ_x, σ_y = stress in the x and y directions, respectively

τ_{xy} = shearing stress in the (x,y) plane

d_5 = constant

The shearing forces are proportional to x along the longitudinal sides and follow a parabolic law at x = 1.

The equations may be used in residual stress analysis only if it is realized that they apply to changes that take place when the cone is cut and may not measure the "absolute" residual stresses. Since the major stresses present in the cone will probably be σ_x and σ_z, and an apparent σ_y will develop from the combined stresses upon cutting the cone, we may use the procedure illustrated in Figure 10 to analyze the stress pattern. If the cuts are made carefully to avoid heating, the deflection resulting in the cut section may be assumed to result from an apparent normal stress in the y direction. Cuts made in the x and z directions and strain measurements in those directions will provide information for obtaining the magnitude of the shearing stress that may be present.

Using the equations:

$$\epsilon_x = \frac{\sigma_x}{E} - \frac{v\,\sigma_z}{E} \qquad (5)$$

$$\epsilon_z = \frac{\sigma_z}{E} - \frac{v\,\sigma_x}{E} \qquad (6)$$

where:

ϵ_x = strain in the x direction

ϵ_z = strain in the z direction

E = Young's Modulus = 17×10^6 p.s.i. for copper

v = Poisson's Ratio = 0.35 for copper
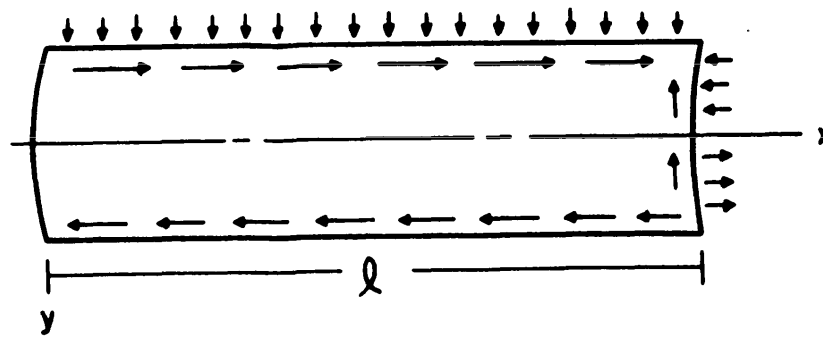
FIG. 9 - STRESS SYSTEM USED FOR CALCULATING RESIDUAL SHEARING STRESSES.
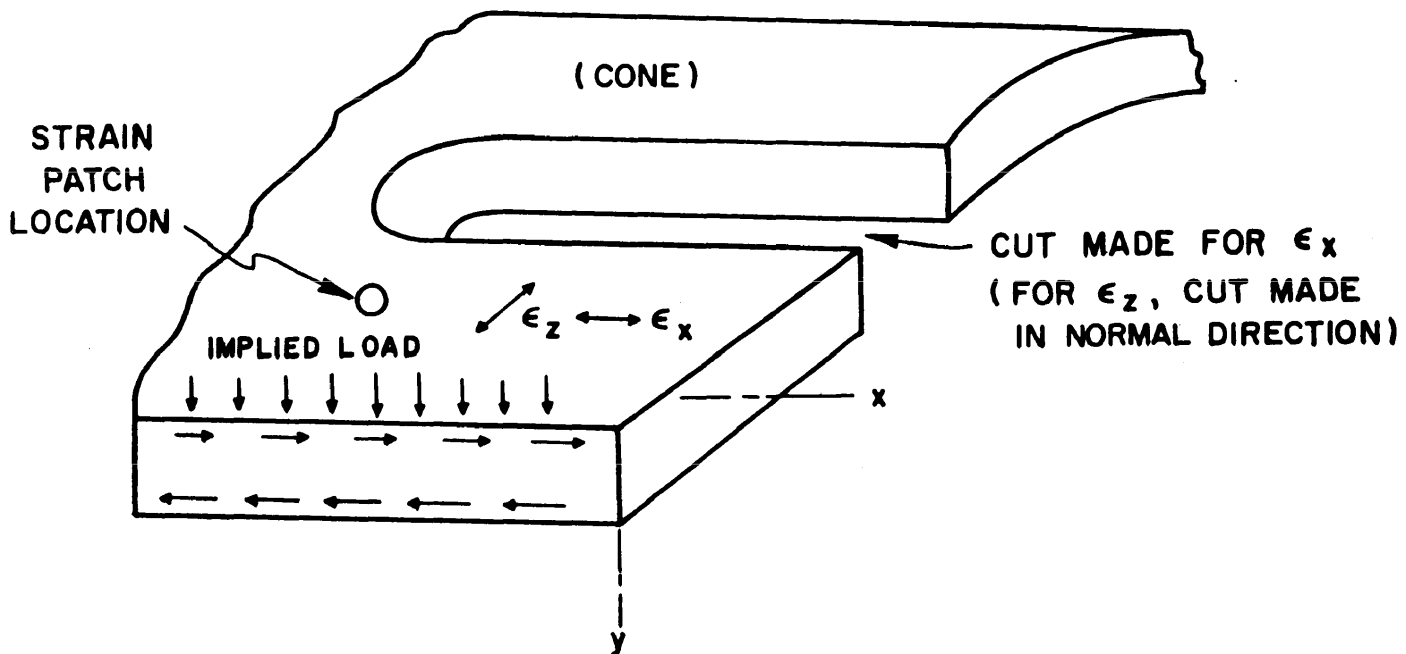
FIG. 10 - STRESS SYSTEM APPLIED TO CONE WALL

σ_x, σ_z, are the stresses in the $\underline{x}$ and $\underline{z}$ direction, as before, and measuring the strains ϵ_x and ϵ_z, the stress in the $\underline{x}$ direction may be found. This value is then substituted into equation (2) and, knowing the position where the measurement is made so that the values for $\underline{x}$ and $\underline{y}$ are known, the constant d_5 may be found. This constant is then used to solve equation (4) for the shearing stress, τ_{xy}.

From this analysis an "order-of-magnitude" value of shearing stress may be found for comparison with the values of shearing stress required by the Carrier and Prager analysis.

2. <u>Experimental Procedure and Results</u>. The results obtained in the strain measurements must be related to the spin compensation of the liner used. This requires either assuming the spin compensation is the same from the base to the apex of the liner and therefore the residual stress varies, or the residual stress is the same from the base to the apex and the spin compensation varies. In either case, results must be interpreted with respect to the position on the liner at which the measurements were made.

a. <u>Rosette Pattern Measurements</u>. A preliminary series of experiments was run to determine the maximum residual shearing stress in the surface of the cone. A rosette pattern of strain gages, as shown in Figure 11, was placed on rotary extruded cones from a group not in the series A-K discussed in this report. Three cuts were made in the cone and the strains measured after each cut. Three different cones were tested, and (using a Mohr's circle solution) the residual stress in the cone surface is determined.

The maximum residual shearing stress determined in this way is 722.5 psi.

b. <u>Strain Gage Measurements of Vertical and Horizontal Strains</u>. On the basis of the theoretical approach described in the previous section, and since the rosette pattern measurements indicated the probable presence of a measurable stress, cones from Lots B, D, and J were tested

FIG. 11—ARRANGEMENT FOR RESIDUAL STRESS
MEASUREMENTS WITH STRAIN GAGES—
(ROSETTE PATTERN)

to determine the residual strains in the $\underline{x}$ and $\underline{z}$ directions. Cuts were made in the cone wall to allow measurement of strain with strain gages, and equations (2) through (6) were used to calculate the shearing stresses.

In addition, using equation (1) the residual shearing stresses required by the Carrier and Prager analysis in cones from Lots B, D, and J may be calculated.

This work was carried out, and the calculated and measured values are shown in Table II.

Table II

Comparison of Experimental and Theoretical Residual Shearing Stresses(τ_{xy})

Cone Lot	σ_x Experimental	τ_{xy} From σ_x	τ_{xy} Experimental	τ_{xy} From Carrier and Prager	Spin Compensation
B	1130 psi	56 psi		764 psi	-20 rps
D	530 psi	27 psi		340 psi	+10 rps
J	1560 psi	78 psi		900 psi	+25 rps

The values used for these calculations in equations (2) through (4) are: $\underline{X}$ = 1 inch and $\underline{Y}$ = 0.050 inches.

Two sources of error are apparent: the first being the two-dimensional analysis used in the calculations although this will be in error by a factor of $(1 - v^2)$ only; the second is the integrating effect of the strain gages. The assumption of a load in the $\underline{y}$ direction, which is used to create a shearing stress similar to the one assumed by Carrier and Prager, requires only a very small load in the cases considered and introduces no more error than their assumptions. The heating effect on the cones does not remove all stresses during manufacture, but undoubtedly reduces them considerably.

The results of the residual stress investigations indicate
that the shearing stresses are too low to cause the observed spin
compensations. Experimental investigations, reported in the next
section, confirmed these observations.

3. Annealing Experiments to Check the Effect of Residual Stress.
To check the conclusion that the residual stress is unimportant in spin
compensation, a series of experiments was devised to determine the effect
of the residual stresses on spin compensation without actually measuring
the magnitude of the stresses.

During the annealing of a cold-worked metal, three changes
occur in the material: recovery (with polygonization following or
occurring at the same time); recrystallization; and grain growth.
Recovery may be looked upon as a low temperature re-adjustment of the
atomic structure that effectively eliminates the residual macro-stresses
in the material without changing the crystal arrangement. Therefore,
during recovery, the same preferred orientation and grain shape and
distribution are retained. During recrystallization, new grains and
new preferred orientations are formed, and remaining local microstresses
are eliminated. During grain growth, certain grains become large at the
expense of the rest. Figure 12 is a schematic representation of the
change of macro-stresses in the material with temperature.

During the cold reduction of dead-soft OFHC copper, as occurs
in the rotary-extrusion process, the material attains a near-maximum
hardness within the first 15-20% of the reduction. The hardness is
related directly to the residual macro-stresses in the metal, and a
hardness-temperature curve would look very similar to Figure 12. By
proper annealing, the residual macro-stresses may be effectively reduced
to zero without changing the material as far as structure, preferred
orientation, etc. are concerned. Annealing cycles were determined for
cones from several lots of liners, and the structure was checked using

STRESS

ZERO MACRO-STRESS BELOW HERE

RECRYSTALLIZATION
BEGINNING

RECRYSTALLIZATION
COMPLETE
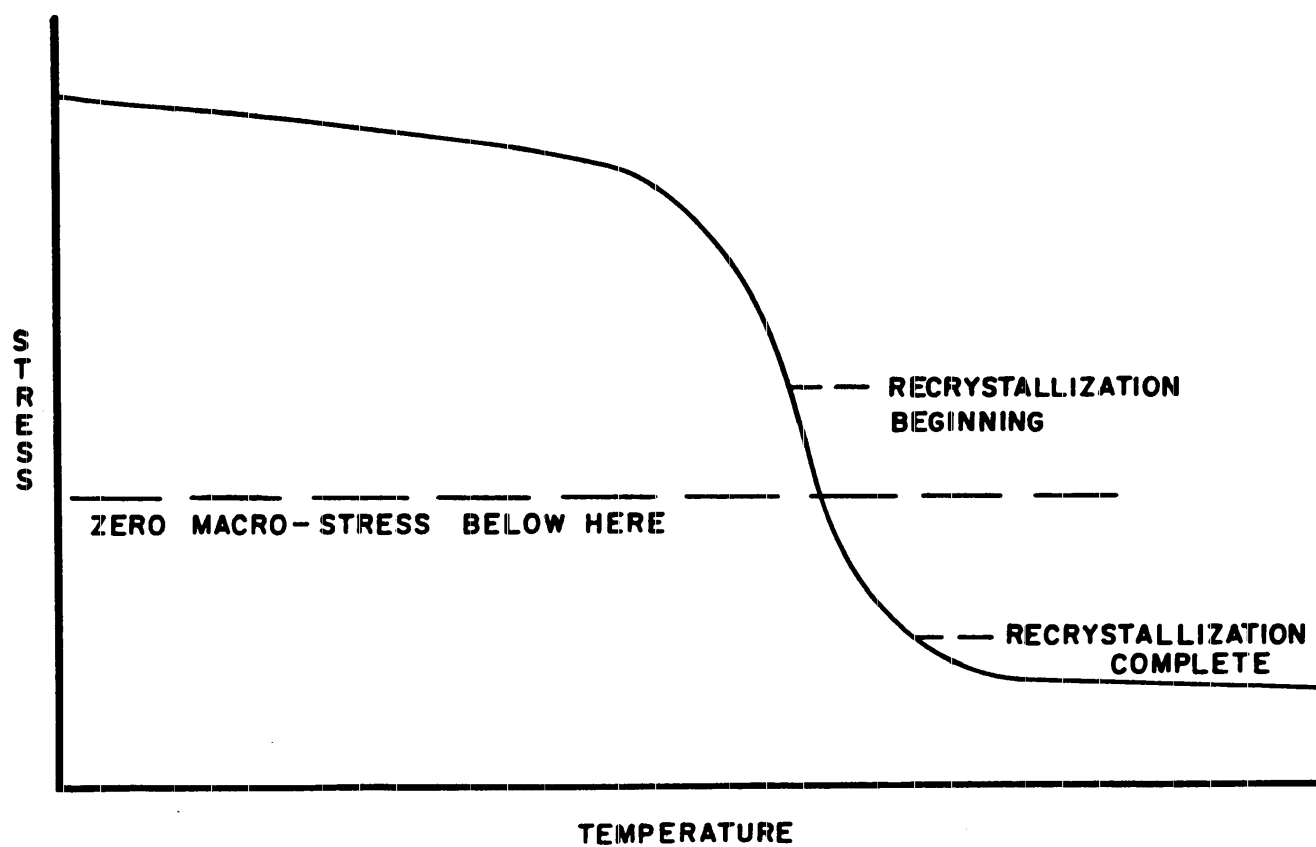
TEMPERATURE

FIG. 12 — STRESS-TEMPERATURE VARIATIONS IN A METAL

X-rays and optical methods to determine the points where changes began. From these data, hardness-temperature curves were established for several lots of cones. Table III shows the data for cones from Lot A.

Table III

Results of Annealing Liners from Lot A for 1/2 Hour

Annealing Temperature $^\circ F$	Rockwell "F" Hardness	X-ray and Metallographic Data
325	85	No change in preferred orientation-no change in the grain structure or impurity distribution
370	84	
410	84	"
460	81	"
500	70	"
525	65	"
545	52	"
555	50	Slight change in preferred orientation thru break-up of the heavy density regions; beginning of recrystallization.
575	47	
600	33	Recrystallization complete; no trace of previous orientation; grain shapes and impurity distribution changed.
625	32	
720	31	

The time of the anneal was 1/2 hour at each temperature. The temperature was controlled within 5 degrees Fahrenheit, and each point represents at least 5 checks of all changes.

Similar data were taken for cones from Lots H and K, and curves similar to that shown in Figure 13, of hardness vs temperature, were plotted.
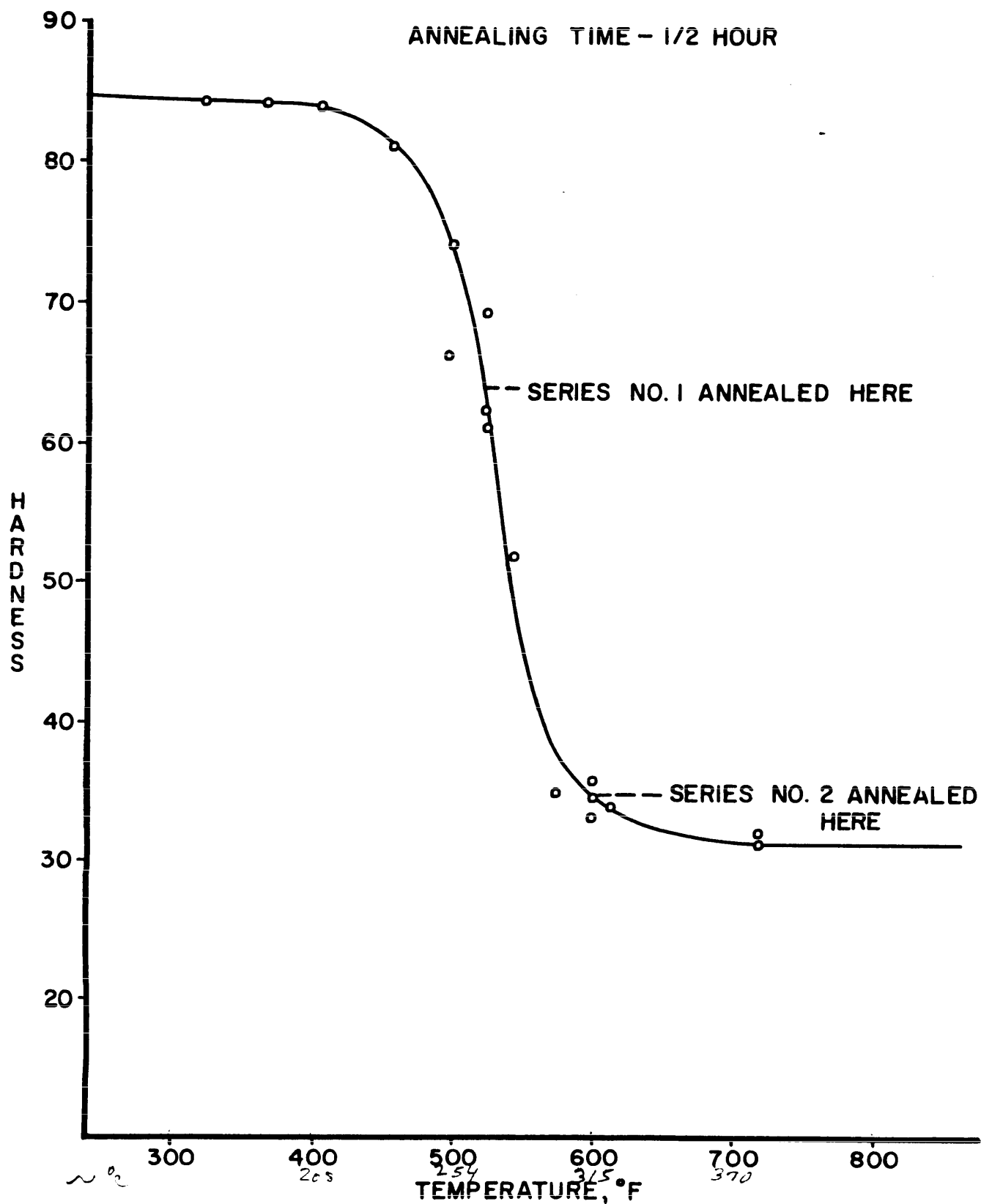
FIG. 13—HARDNESS-TEMPERATURE VARIATION IN
CONE FROM LOT "A"

Using these data, cones from Lots A, H, and K were annealed at two different temperatures: a low temperature that would eliminate the residual macro-stresses without changing the structure, and an elevated temperature that would change the structure. These two temperatures are noted for cones from Lot A on the curve in Figure 13. The cones were then tested to determine their spin-compensation frequencies. The results were as follows:

> (1) The cones annealed below the recrystallization temperature, to remove the residual stresses only, showed no change in spin-compensation frequency.

> (2) The cones annealed above the recrystallization, temperature to produce structural changes, showed a total loss of spin compensation, performing as normal, deep-drawn liners.

These results were true for all lots of liners tested.

3. Conclusions. From the preceding experiments, the following conclusions are drawn:

a. The residual stresses make no significant contribution to the spin-compensation properties of the liner. The spin compensation appears to be related to a structure property.

b. The residual stresses present are small in comparison to those needed to produce a spin-compensation frequency of the magnitude observed. It should be pointed out that for residual stresses to affect the spin compensation of a liner they would have to be of such a magnitude as to give the cancellation of spin frequency during the time of the collapse on the liner, and their effect should be felt before the liner reaches the jet axis.

c. Shearing stresses in a spun liner of the type discussed would produce a variable spin frequency from base to apex, unless they vary linearly from base to apex themselves; neither was observed.

Since the spin compensation is apparently associated with a
structure property, the effects of grain size and shape, impurity
distribution, etc. were investigated and are discussed in the next
section.

C. Metallographic Examination

1. _Theory_. The metal flow during the forming process causes a
reorientation and change in shape of the grains in the metal, and a
redistribution of the impurities and grains with respect to the
surfaces of the cone. An analysis of the metal flow has been made
which indicates that the relative movements of the material near the
two cone surfaces are in opposite directions, and that the material
between the two surfaces is under the influence of a severe shearing
force. Plastic flow during the reduction of the thickness of the
blank, and the forming of the cone, carries material down the mandrel
(Figure 4), but the reorientation of the grain structure in the cone
is opposite to that which would be expected to result from the friction
between the tool and the copper blank. The copper has been reduced
60% in the forming.

By assuming that the collapse of metal in the liner under
detonation loading will follow, to at least a slight degree, the path
of least resistance, paths of weakness were looked for metallographically.
Since the grain boundaries are normally considered regions of high
strength compared to the grains, at room temperature, it is possible
to imagine an arrangement of grains such as that shown schematically
in Figure 14, where easy collapse paths are present along the grain
boundaries or along the grains. This would give a preferred flow
direction to the element of liner as it collapses, so that a component
of the collapse would be directed normal to the radius vector. This
component would cause a rotation to be given to the metal as it
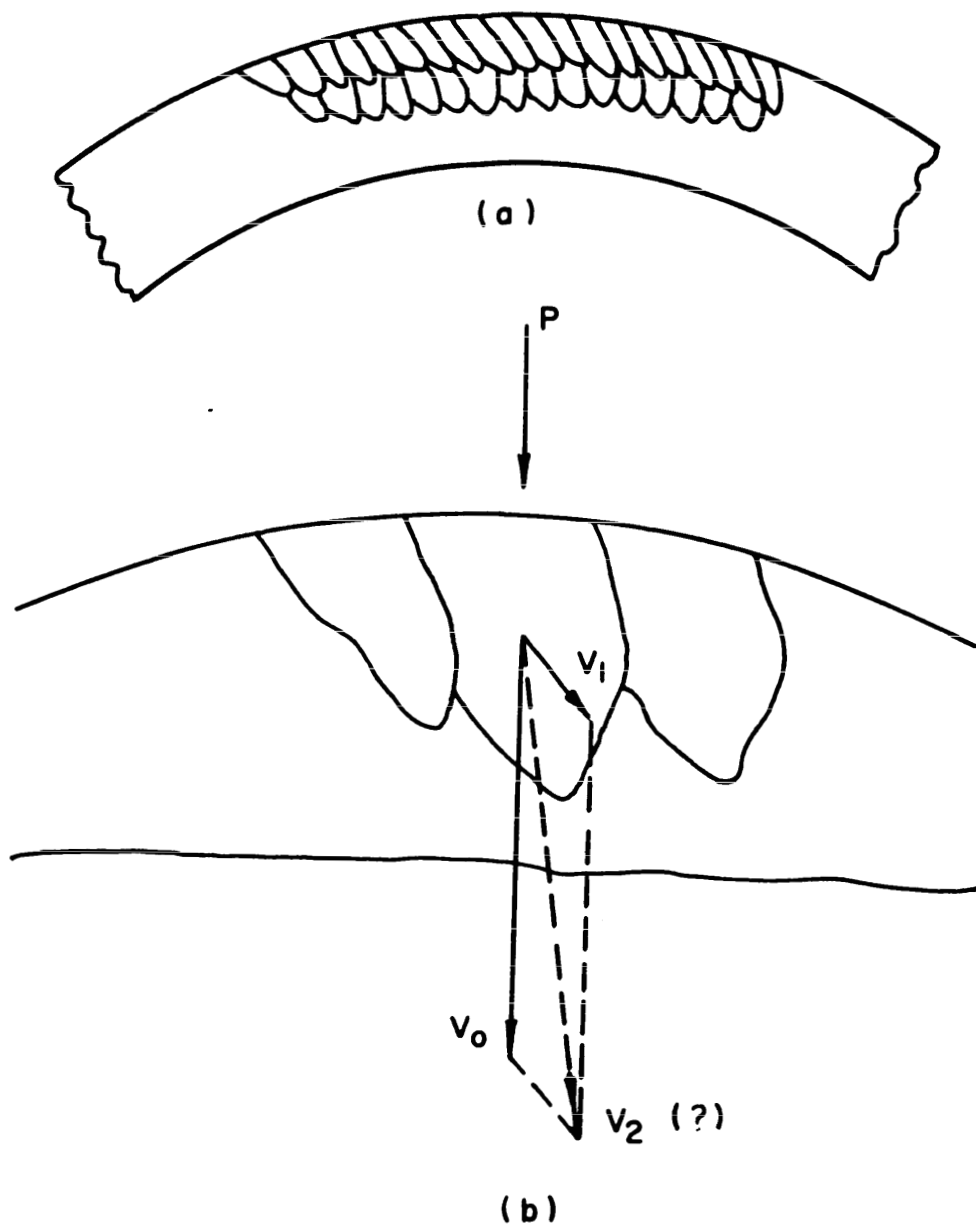collapsed. It is not important that the macro-effect of this tangential

37

(a)

(b)

FIG. 14-SCHEMATIC OF ORIENTED GRAIN STRUCTURE

flow carry thru the cone wall, since any initial tangential flow will probably persist through the collapse process. Surface effects could create the necessary tangential component of velocity if they are strong enough.

Similarly, the alignment of non-metallic inclusions, which are harder than the base metal, could create difficult and easy paths of collapse which would cause a rotation in the jet. Any physical change in the arrangement of the metal substructure that produced paths of easy collapse would offer an explanation for the "built-in" spin compensation found in shear-formed liners. In the following sections these factors are investigated by metallographic methods and the results are noted.

2. Experimental Procedure and Results.

a. Grain Structure. Metallographic studies were made of the cones from each lot, using standard techniques and etchants. Longitudinal and transverse samples were taken in different places on the cones to insure adequate coverage. Figure 15a, is a photomicrograph of the blank metal before forming. Figure 15b, shows the structure of a cone at the outer surface, and Figure 15c, is a micrograph of the same cone 3/4 ths of the wall thickness from the outer surface. All micrographs were taken from transverse sections. Referring to Figure 15, it will be seen that the cone forming process has deformed the outer surface of the cone very heavily. The elongated grains seen in Figure 15b, are representative of all cone lots. The structure of the cone metal near the inner wall shows the effect of the deformation, but the effect is slight compared to that near the outer wall. Between the two types of structure represented by Figures 15b and c, there is a transition region from the very heavily worked metal to the more normal structure and it is difficult to determine the exact separation line between the two regions.
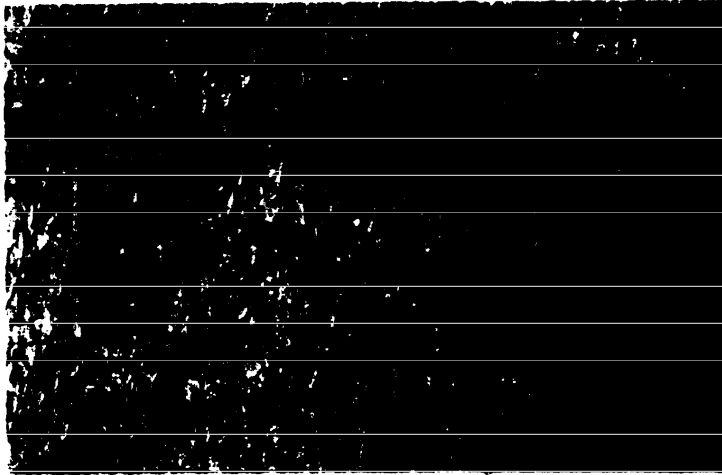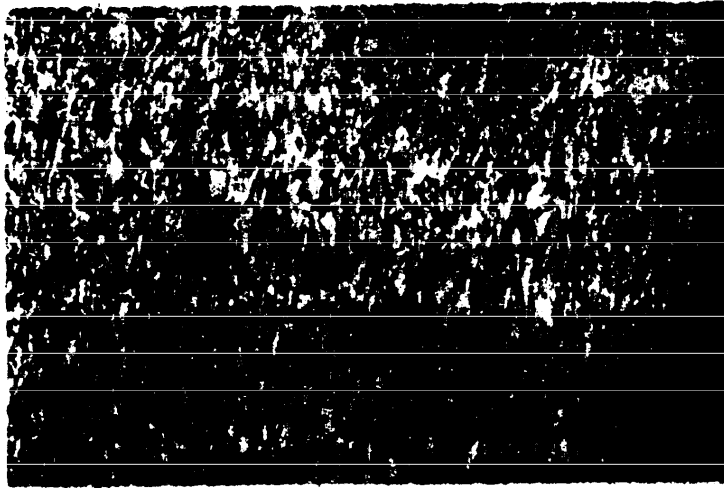
c.—INNER CONE WALL

b.—OUTER CONE WALL
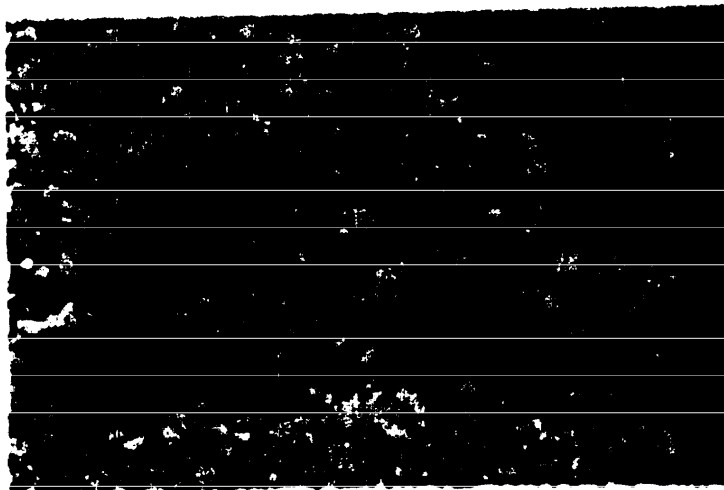
a.—BLANK MATERIAL

FIG. 15.—PHOTOMICROGRAPHS OF THE COPPER BLANK AND CONE MATERIAL.— 200 X MAGNIFICATION.

The depth of the heavily worked region varies from one lot of cones to the next, as may be seen in Table IV. These measurements include the transition zone, the thickness of which is more variable than the outer zone of heavily distorted grains. The depths are plotted in Figure 16 as a function of spin compensation frequency.

Table IV

Combined Depth of Cold Worked Layer and Transition Zone in Spun Liners

Cone Lot	Depth of Layers (inches)	Spin Frequency (cps)
A	0.030	-25
B	.020	-20
C	.019	-8
D	.022	+10
E	.026	+10
F	.030	+15
G	.030	+20
H	.036	+22
I	.036	+25
J	.039	+25
K	.041	+35

To determine the effect of this cold-worked region on the spin-compensation frequency, as compared to the normal structure in the rest of the cone, metal was removed from the outer and inner surfaces of cones from different lots, and their spin-compensation frequencies determined. Results from these tests are reported for Cone Lot H in Table VIII. The results are also typical of those from the Lots A and K.

41
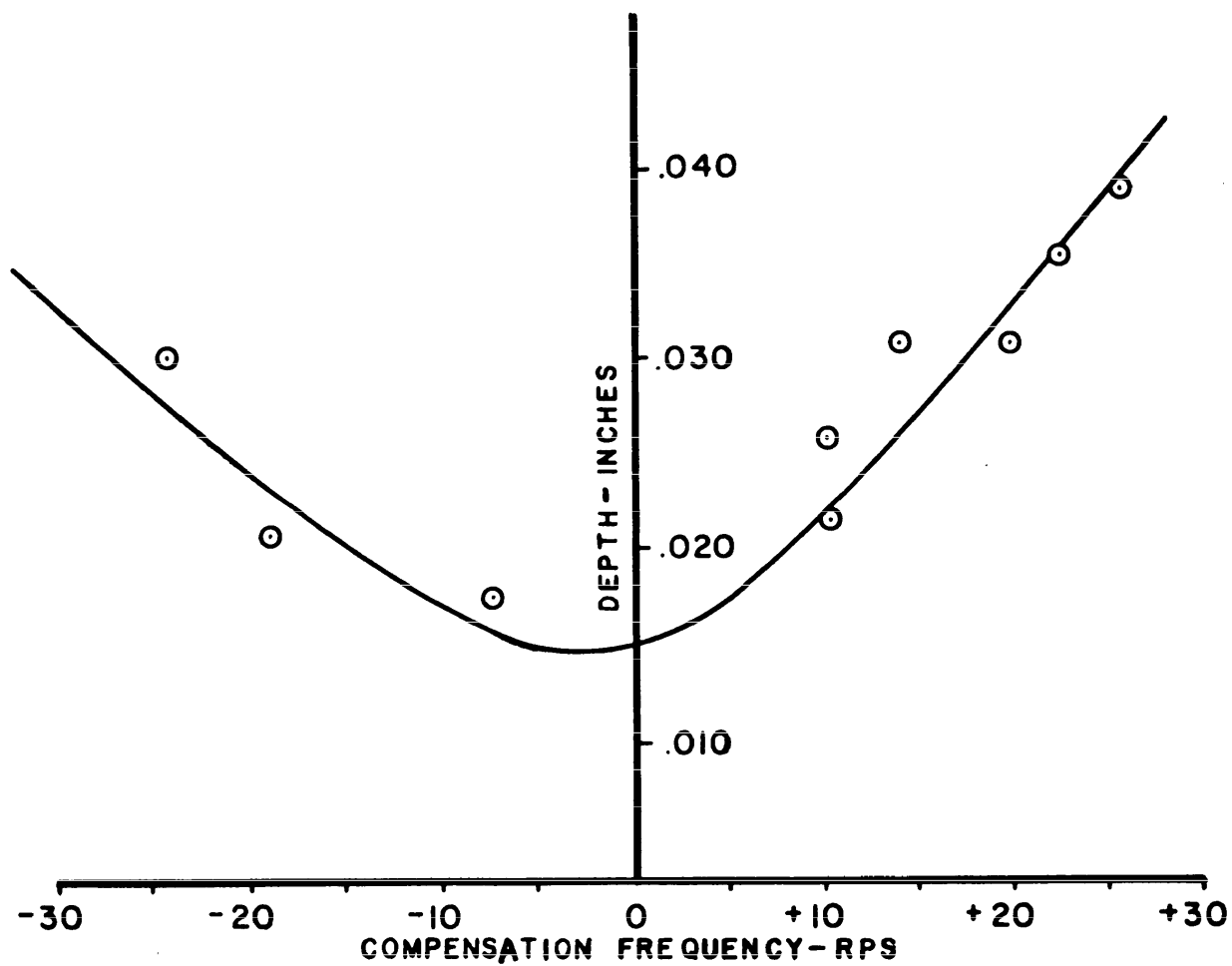
FIG. 16 - SPIN COMPENSATION vs. DEPTH OF
COLD WORKED LAYER

Table V

Effect on Spin Compensation Frequency
of Removing Metal from Liners of Lot H

Treatment	Spin Frequency (cps)
a. Normal, no metal removed from either wall	+22
b. 0.015 inches metal removed from the outer wall	+22
c. 0.030 inches metal removed from the outer wall	+22
d. 0.020 inches metal removed from the inner wall	0 to +5
e. 0.030 inches metal removed from the inner wall	0

While the loss of the outer, heavily-worked regions in the cones has no apparent effect on the spin-compensation frequency, the loss of metal from the inner wall completely removes the spin-compensation effect.

    b. Other Observations.

No consistent variation of any other parameter with the spin compensation frequency was observed using metallographic techniques. Although the cones are reportedly OFHC copper, there is a large amount of copper oxide distributed throughout the metal. A consistent pattern of distribution of the oxide was not observed to change with spin compensation frequency.

Under heavy etching with 1:1 HNO_3, a series of strain lines were observed that followed the pattern formed on a cone when a network of lines is scribed on the blank, as described previously. Again, no useful variation of these strain markings was observed from one lot of cones to another.

3. Conclusions. The following conclusions are drawn from the results of the metallographic investigation:

    a. The heavily cold-worked layer on the outer surface of the cones from a given lot does not cause "built-in" spin compensation.

    b. The presence of inclusions or strain-flow markings does not contribute to spin compensation.

    c. Residual shearing stresses do not produce spin compensation since the removal of metal from the outer and inner walls has different effects.

    d. The spin compensation probably arises from an intrinsic property of the metal, such as a variation in crystallography, since the removal of the metal from the inner surface decreases the spin compensation.

With the above in mind, a systematic investigation of the crystal structure was carried out, using X-ray diffraction techniques. This investigation is reported in the following section.

D. Preferred Orientation Studies

1. Theory. Copper is a face-centered cubic material, having no known low-temperature or high-temperature allotropic transformations. The only variation possible in a polycrystalline specimen is the lack of complete randomness in the orientation of the grains of the metal. If the grains are of similar orientations, a number of planes of the same type will lie in a preferred direction with respect to the surface. This "preferred orientation" may be studied thru the use of X-ray diffraction techniques. These methods depend upon very precise experimental work for measuring intensities of diffracted X-ray beams.

The specimens used are either small solid cylinders of metal, machined from the section to be studied, or flat specimens. Both back-reflection and transmission patterns are usually taken with the

flat specimens to cover the necessary range of angles between X-ray beam and the specimen. Figure 17 illustrates the technique used, where an X-ray beam impinges on a metal specimen and the beam diffracted from an atomic plane satisfies the Bragg relationship of

$$n\lambda = 2d \, \sin\Theta \tag{7}$$

where λ = wave length of the X-rays

           d = spacing between atomic planes

           Θ = angle of diffraction between the X-ray beam and the atomic plane

           n = an integer, generally 1 in this work

The diffracted X-ray beam either passes through the specimen, giving a transmission pattern on an X-ray film suitably placed, or is reflected back from the plane to an X-ray film through which the X-ray beam has passed originally, giving a back-reflection pattern, as shown in Figure 17. The experimental arrangement depends on the various values of the parameters in Bragg's law, and the metal section to be investigated.

As seen in Figure 17, the diffracted ray from one plane at one point in the X-ray beam, maintaining the angle Θ, will cause one spot on the X-ray film. If there is random orientation of the grains in the metal covered by the area of the X-ray beam, a cone of diffracted rays coming from all of the possible orientations of a given plane making the angle Θ with the X-ray beam, will cut the X-ray film in a circle. This diffraction ring will have uniform intensity for random grain orientation, but if the atomic planes tend to be oriented in one direction, the intensity will become greater in one part of the ring and less at others. Therefore, the variation of the intensity around the diffraction ring is a suitable measure of departures from randomness in the distribution of the crystal orientation in the metal.
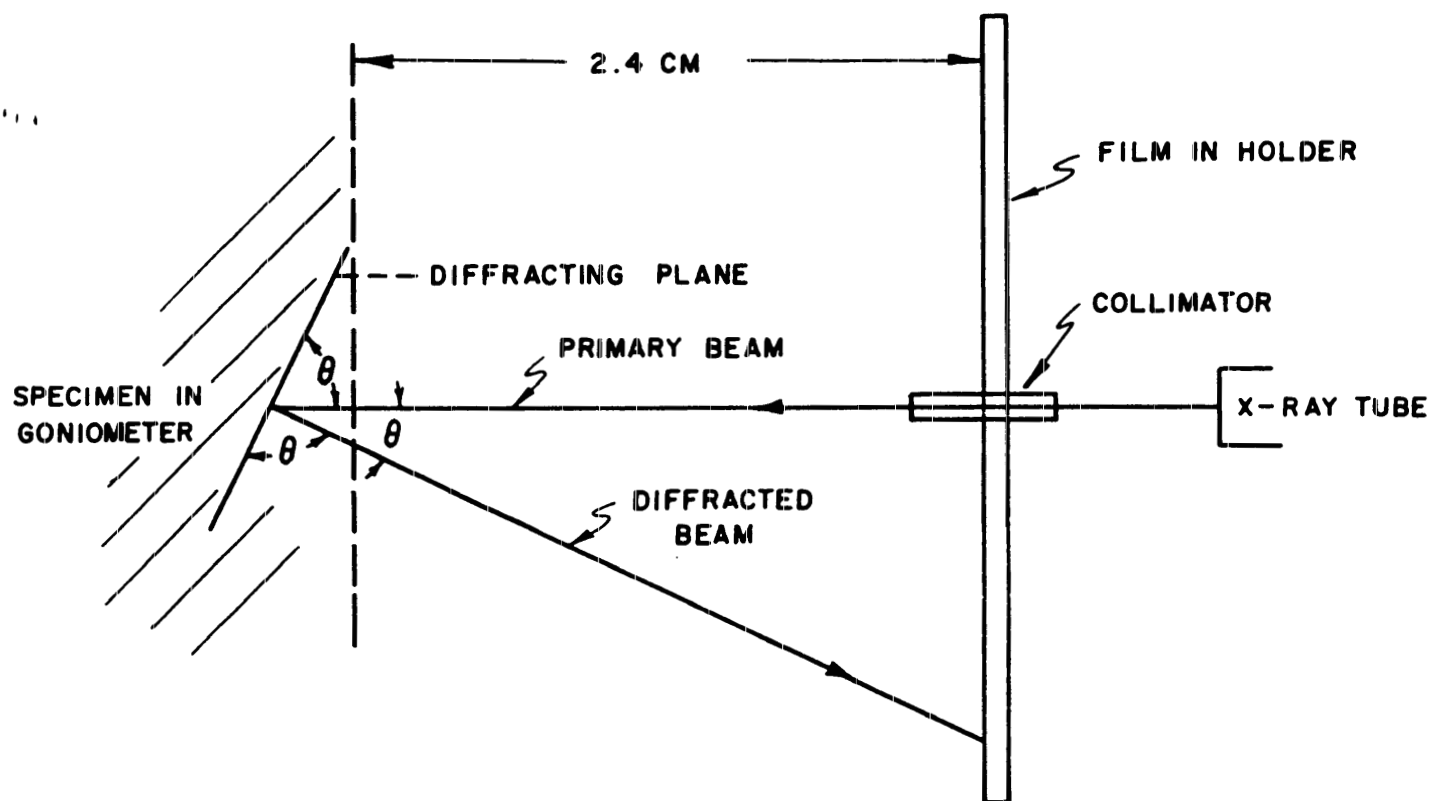
FIG. 17 — ARRANGEMENT FOR TAKING A BACK REFLECTION
X-RAY PATTERN

When a metal has undergone plastic flow, the random orientation of the grains is generally destroyed and the grains try to align themselves in some configuration that depends on the crystal structure of the metal and the nature of the deformation process. The manner in which a given atomic plane is aligned with respect to some axis in the specimen is called the "texture pattern", and this pattern is consistent for all specimens of a given metal if conditions of deformation are held constant.

Since metal deformation under standard conditions follows definite directions on specific crystal planes, a preferred orientation or "texture" in a piece of metal determines the mode of failure of that specimen. This accounts for preferred flow directions in worked metals, and could possibly explain the presence of a preferred flow direction in the rotary-extruded liners that exhibit spin compensation, if the metal deforms crystallographically under detonation loading. Evidence that the crystal structure influences collapse of a liner was found in the firings of single-crystal liners mentioned in Section II - b of this report. The presence of a preferred orientation of a plane along which the metal flows easily in the cone wall could produce a tangential component of metal collapse giving rise to spin compensation, as discussed in Section II and following the schematic in Figure 14. The magnitude of the rotation will depend on the magnitude of the tangential flow component imparted to the material forming the jet.

It was therefore necessary to determine the following:

a. If a preferred orientation, or texture pattern, exists in the copper liners, and, if it does;

b. The variations of the orientation with position in the cone, (if any).

c. The variation of the amount of preferred orientation with the spin-compensation frequency, (if any).

d. An explanation for the flow patterns that could arise from the preferred orientation.

2. _Experimental Procedures and Results._ The techniques used in examining the preferred orientation in these liners differ from standard quantitative practices for a number of reasons, most of which are concerned with the nature of the specimen under study. Since the $\{111\}$ plane is the slip plane in copper (see Figure 18) under normal conditions, it would be best to work with this plane. However, to do so, transmission diffraction patterns would have to be used, which would necessitate the use of very thin specimens or special back-reflection techniques would have to be employed.

Since several hundred X-ray shots were necessary for surveying the cones from each lot, it was impracticable to prepare special specimens involving lengthy etching. The specimens could not be machined, since this would impose cold work on them and alter the surface layers being studied. The curved surfaces of the specimens cause a broadening of the diffracted X-ray beam, and any attempt to flatten a specimen out from the cone would naturally change the results. In addition, the technique of using a cylindrical specimen machined from the cone wall would remove the possibility of determining any change in orientation from the outer to the inner cone wall. Therefore, the following procedure was used in this study:

a. Collimated $C_r K_\alpha$ radiation was used in the back-reflection technique. Measurements of intensity and angles were made with a microdensitometer on the $\{220\}$ plane, hereafter referred to as the $\{110\}$ plane.

b. The specimen holder held the entire cone, and allowed for three-circle adjustment - i.e., rotation of the cone about three axes. Longitudinal and lateral rotation of the specimen about mutually perpendicular axes through the point where the X-ray beam hit the cone was provided for, the two axes forming an orthogonal, triaxial system with the X-ray beam as the third axis.
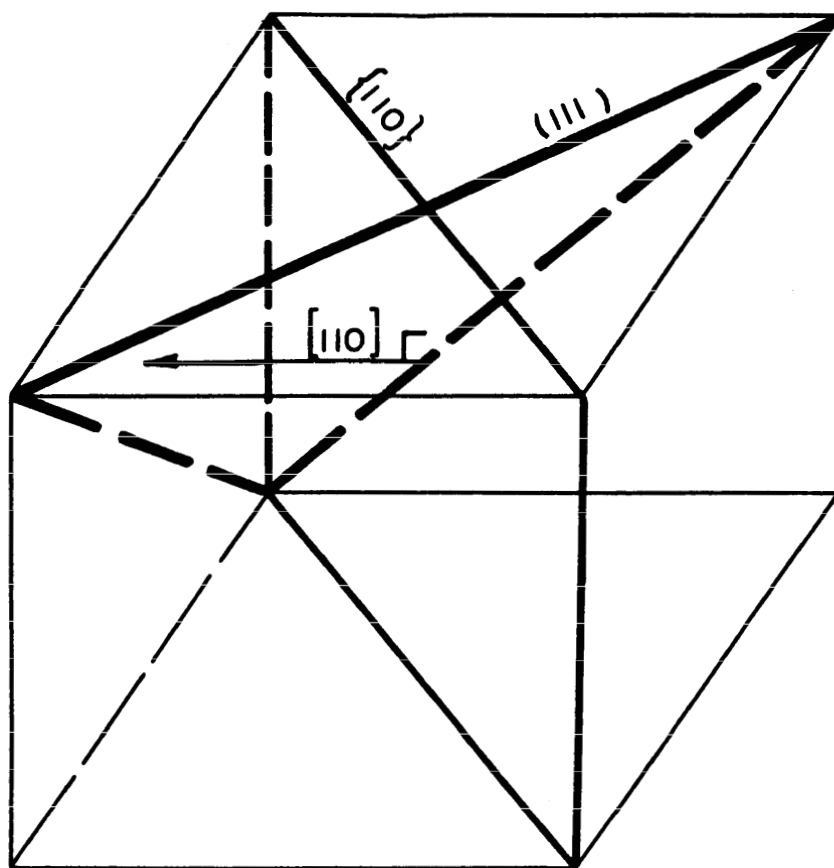
FIG. 18 — THE {110} AND {111} TYPE PLANES IN COPPER
WITH THE [110] DIRECTION IN THE (111) PLANE

c. Cones from different lots were X-rayed at various points on the surface of each cone. Material was then etched from the outside of the cone and the process repeated.

d. Pole figures (plots of the texture pattern, or preferred orientation, as it varies around the axial system described in b above) were plotted for selected points in different lots of cones.

e. All variables, such as development of the X-ray film, etc., were maintained constant from experiment to experiment.

f. Intensity measurements were made on the film to determine if a numerical correlation between preferred orientation and spin frequency existed.

g. Intensity absorption correction data were determined for the X-ray diffraction pictures taken at various angles of incidence between the X-ray beam and the specimen.

(1) Survey of the liner surface.

Initially, a cone from Lot A was examined at 0.004" below the surface. X-ray patterns, with the X-ray beam at normal incidence to the liner surface, were made every 60° around the cone and every 1/2" from the base to the apex. The patterns obtained were similar in all cases except very near the base of the cone and at the apex. Cones from other lots were checked at six points on the surface and no change in the pattern of the individual lots was found from one point to the next on a given liner.

(2) Survey of different lots of liners at normal incidence.

A point one inch from the base of a liner was chosen as the standard region to be examined, and normal incidence X-ray diffraction patterns were made of Cone Lots A through K at this point, 0.004" below the outer surface. A preferred orientation of the $\{110\}$ plane was found in each cone which was different for each cone lot. Figure 19 shows the diffraction rings for cones from several lots of
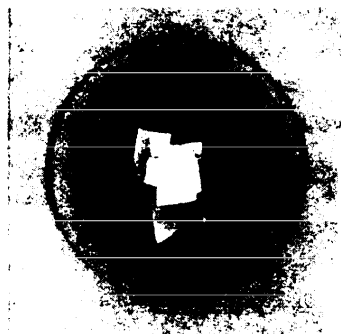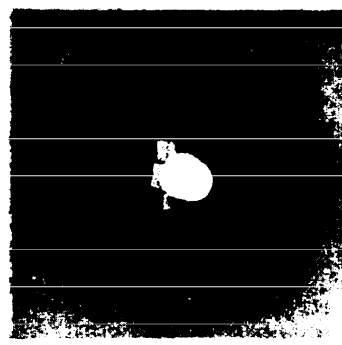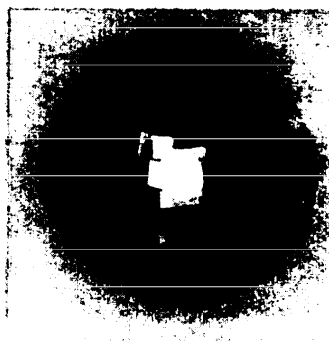
a. b. e.

f. g. j

FIG. 19 — NORMAL INCIDENCE X-RAY DIFFRACTION
PATTERNS OF DIFFERENT CONE LOTS.
(LOT IDENTIFICATIONS
APPEAR UNDER FIGURES)

liners. It may be seen that the intensity varies around a given ring with distinct maxima and minima. The diffraction rings were laid off as seen schematically in Figure 20, where the angles δ_1 & δ_2 represent the angles from the horizontal to the points of maximum intensity on either side of the diffraction ring. Table VI shows the data for the X-ray observations taken with the incident beam of X-rays perpendicular to the liner wall. The columns labeled "Intensity Spread" indicate the width of the regions of maximum intensity. " ($I\delta_1$ - $I\delta_2$) " is the difference in intensity of the two intensity maxima observed on the film. The units of intensity measurement used are percent light transmitted through the film, corrected for background film density. Therefore, the greater the intensity number, the weaker the diffracted beam of X-rays, or the lighter the film.

A correlation is readily seen between the spin compensation frequency and ($I\delta_1$ - $I\delta_2$) . This is plotted in Figure 21 and discussed in a later section.
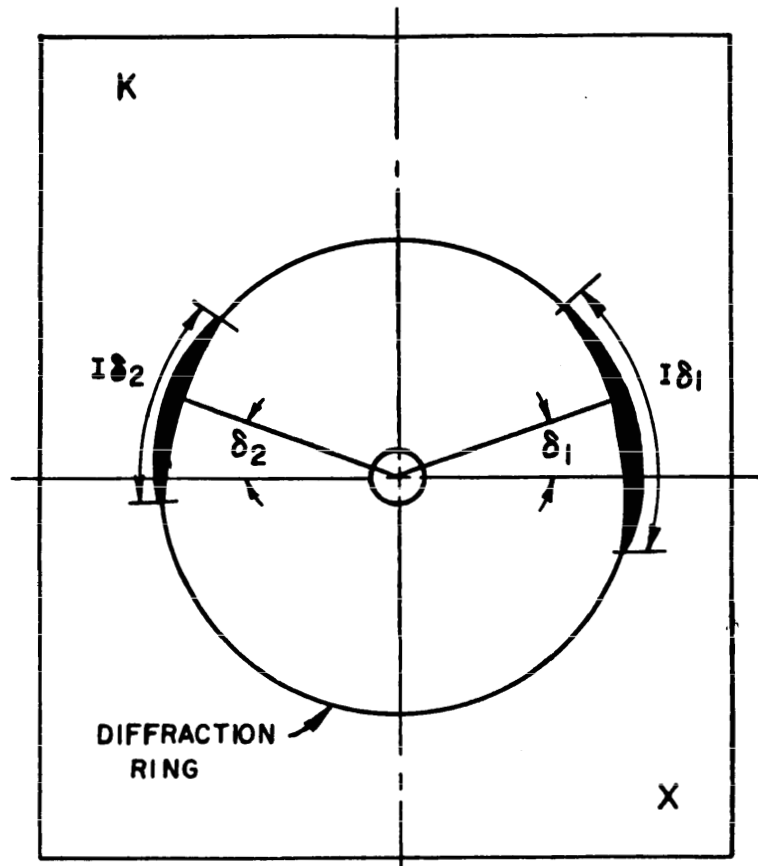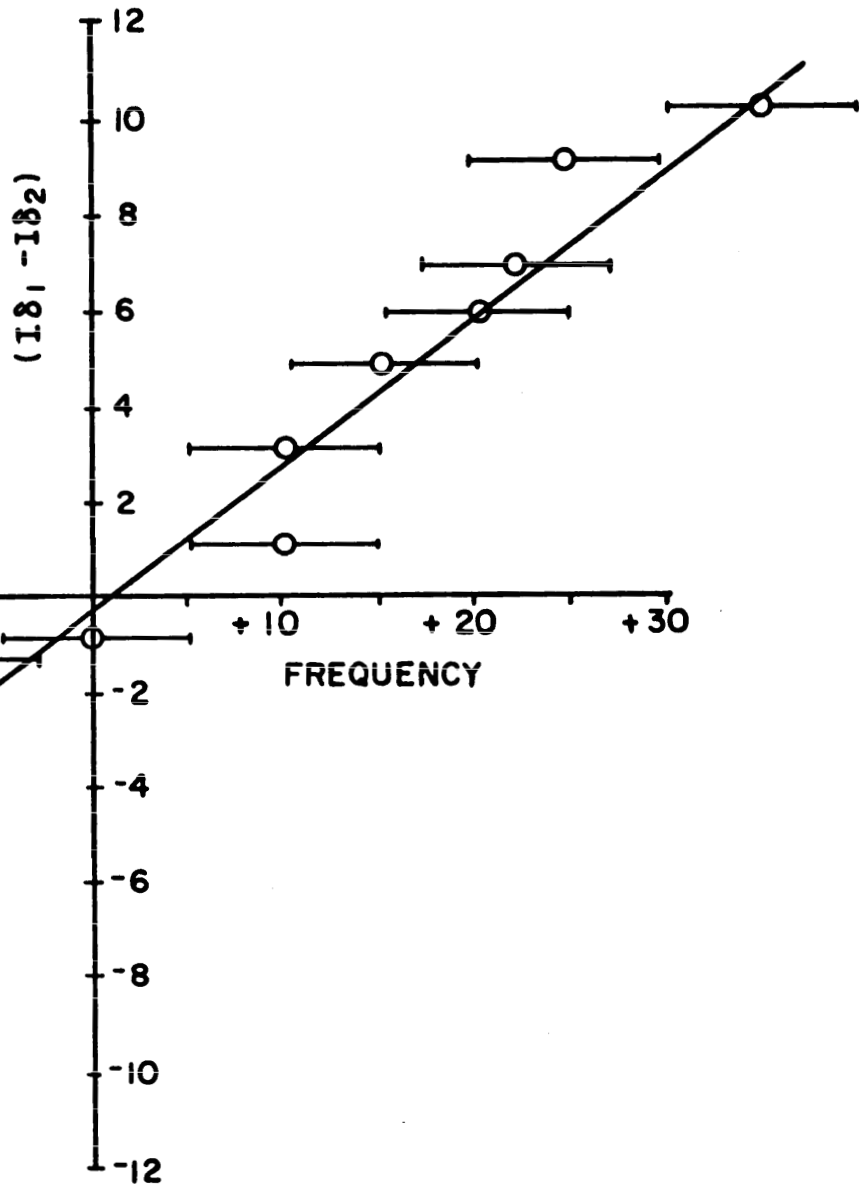
FIG. 20 —MEASUREMENTS TAKEN ON
X-RAY PATTERNS

FIG. 21—DIFFERENCE IN INTENSITY MAXIMA vs. SPIN FREQUENCY
FOR NORMAL INCIDENCE X-RAY PATTERNS

Table VI

Intensity Data from Normal Incidence X-ray Patterns

Cone Lot	δ_1	Intensity Spread	δ_2	Intensity Spread	$I\delta_1 - I\delta_2$	Spin Comp. Frequency
A	$0°$	$\pm 10°$	$0°$	$\pm 2°$	-8	-25 rps
B	0	± 5	0	± 2	-3	-20
C	0	± 2	-15	± 2	-1	-8
D	0	± 2	$+15$	± 2	$+1$	$+10$
E	0	± 2	$+15$	± 2	$+3$	$+10$
F	-5	± 2	$+15$	± 2	$+5$	$+15$
G	0	± 2	0	± 2	$+6$	$+20$
I	0	± 2	-10	± 10	$+7$	$+22$
J	0	± 2	-10	± 10	$+9$	$+25$
K	10	± 2	-20	± 5	$+10$	$+35$
Deep Drawn Liners	-4	± 5	-4	± 5	-1	0

(3) Studies of cone Lots A, C, and K at different depths from the outer surface.

Normal-incidence X-ray patterns were taken at various depths from the outer surface, using cones from Lots A, C, and K. Table VII shows the results from these experiments. Several observations may be made concerning the preferred orientations:

(a) The region of strongly preferred orientation changes from one side of the diffraction ring to the other as X-ray patterns are taken from the outer to the inner wall of the liner, reaching a point where no further change takes place in the inner part of the cone wall.

(b) Cones showing considerable spin compensation also have regions of randomly oriented metal in the outer half of the cone wall.

(c) Cones showing little spin compensation have no region of random orientation. For instance, the cones from Lot C show a reversal in orientation maxima at 0.015" below the outer surface.

Table VII

Data from X-ray Diffraction Patterns Taken at Various Depths from the Outer Surface

Cone Lot	Depth from Outer Surface	δ_1	Intensity Spread	δ_2	Intensity Spread	$I\delta_1 - I\delta_2$
K	0.004"	$0°$	$\pm 2°$	$-10°$	$\pm 10°$	+10
	0.010	0	+10	-10	+10	+ 6
	0.020	-10	+10	+20	+10	- 1
	0.030	- 5	+10	+15	+ 5	- 7
	0.045	+10	+10	+15	+ 5	- 7
	0.065	+10	+10	+15	+ 5	- 7
	0.085	+10	+10	+15	+ 5	- 7
C	0.004"	$+10°$	$\pm 5°$	$-15°$	$\pm 2°$	- 1
	0.015	+10	+ 5	-15	+ 5	+ 2
	0.025	+10	+ 5	-15	+ 5	+ 2
	0.040	+10	+ 5	-15	+ 5	+ 2
	0.060	+10	+ 5	-10	+ 5	+ 2
	0.080	+10	+ 5	-10	+ 5	+ 2
A	0.004"	$0°$	$+10°$	$0°$	$\pm 2°$	- 8
	0.010	0	+10	0	+ 5	- 7
	0.020	0	+10	0	+10	- 2
	0.030	+20	+ 5	0	+10	+ 5
	0.045	+15	+ 5	0	+10	+ 6
	0.065	+15	+ 5	0	+10	+ 6
	0.085	+15	+ 5	0	+10	+ 6
Deep Drawn Liner	0.004"	$- 4°$	$\pm 5°$	$- 8°$	$\pm 5°$	- 1
	0.040	- 4	± 5	- 8	± 5	- 1

(4) Variations in orientation around a point.

Work reported previously was of the survey type, and all X-ray patterns were made with the beam at normal incidence to the cone wall, with the cone axis in a verticle plane. In this section are reported the results of performing rotation studies; i.e., the cone is rotated in 5 degree steps about each of two axes through the point where the X-ray beam strikes the specimen. One axis in the specimen holder allows rotations to the right or left of normal, while the other allows rotations above or below normal. The resultant data may be plotted on a stereographic net and will represent the concentration of the poles of the plane under study at any angle to the cone surface, where the stereographic net represents that surface. These plots are discussed in Part 4 of this Section.

On rotating the cone above and below normal, little change in the intensity distribution was observed. Rotating to the right or left of normal changed the intensity until the distribution between the two maxima became equal. Two observations were made on rotating to the right or left of normal (about a vertical axis):

(a) The points at which $I\delta_1$ and $I\delta_2$ are greatest occur 55 to 60° apart in all cases.

(b) The maximum values of $I\delta_1$ and $I\delta_2$ occur approximately 30° to the right or left of the angle at which $I\delta_1 = I\delta_2$.

In surveying different cone lots, the angle of equal intensity of $I\delta_1$ and $I\delta_2$ was found and then one of the maxima was checked. These data are reported in Table VIII.

Table VIII

Back Reflection X-ray Data on Equal and Maximum
Intensity Distribution for the $\{110\}$ Plane

Cone Lot	Depth	Angle of $I\delta_1$,Max	$I\delta_2$,Max	% Transmission for: $I\delta_1$	$I\delta_2$	$I\delta_1\perp$	$I\delta_2\perp$	Angle at which $I\delta_1 = I\delta_2$
A	0.004"	25-30°R	20-25°L	8	7.0	22.0	14.0	5-10°R
A	0.065	20-25 R	30 L	4.5	4.0		9.0	
A	0.075	20-25 R	25-30 L	4.5	4.0	8.5	9.2	5- 7°R
A	0.085	20-25 R	25-30 L	4.0	3.5	7.0	8.0	0- 3°R
B	0.046	20-25 R	25-30 L	3.5	3.8	6.0	7.5	3- 5°L
C	0.040	20-25 R	25-30 L	11.5	12.0	16.0	18.0	0- 3°L
F	0.040	30 R	20 L	6.5	6.0	15.5	13.0	5°R
J	0.040	35 R	20 L		10.0		19.0	5-10°R
K	0.004	20 R	30 L	3.0	5.5	8.0	18.0	10-15°L

3. <u>Discussion of Results and Conclusions from X-Ray Studies</u>. The X-ray data were obtained under as accurate conditions as could be maintained. Calibration curves, correction factors, etc., were determined and applied to the data. All measurements on the film were made with a micro-densitometer and all films were given the same development treatment. Inaccuracies in the results occur from two sources: (1) small differences between film series that may show up as large differences in reading the films; (2) the specimen shape introduces errors in making X-ray measurements, and rotations of the specimen greater than 50 degrees are prohibited by absorption differences.

However, since the work involved necessitated the use of the original specimen, and goniometric techniques were not readily adaptable to the problem, the techniques used were considered good enough for qualitative comparisons. Interpretation of the various experiments

follows, with conclusions.

a. Intensity data for the $\{110\}$ plane.

(1) <u>Data from Intensity Measurements on Cones A through K</u>. Referring to Table VI and Figure 21, the change in intensity around the back-reflection rings in Cone Lots A through K may be compared on the basis of two intense regions found on the rings. The two regions are referred to by the angles δ_1 and δ_2 defined in Figure 20. The variation in these intense regions may be seen in Figure 19 for the different cone lots in the normal-incidence diffraction patterns taken just below the outer surface of the liner. The deep drawn liner, which shows no spin compensation, has regions of almost equal intensity at δ_1 and δ_2.

Figure 21 is a plot of the difference in intensity in the two regions, $(I\delta_1 - I\delta_2)$, for the normal incidence X-ray patterns, as a function of the spin-compensation frequency. A linear relationship is found that is well within the experimental errors encountered in the flash-X-ray determination of spin frequency and the intensity measurements on the diffraction rings.

(2) <u>Intensity Changes from the Outer to the Inner Wall</u>. Table VII and Figure 22 show the change in $(I\delta_1 - I\delta_2)$ for a given cone, from the outer to the inner wall, for normal incidence studies. The change for cones having little or no spin compensation is very slight, as seen for Cone Lot C. For liners showing large spin compensation, the change is linear to the point where the intensity differences become constant.

(3) <u>Comparisons with Maximum and Equal Intensities</u>. Table IX and Figure 23 show the ratio $I\delta_1/I\delta$ max as a function of spin compensation frequency for the various cone lots where $I\delta_1$ is the maximum intensity of the diffracted beam, with the X-ray beam perpendicular to the cone wall, and $I\delta$ max is the maximum intensity found for the diffracted beam. Figure 24 is a plot of the angle at which $I\delta_1 = I\delta_2$ vs
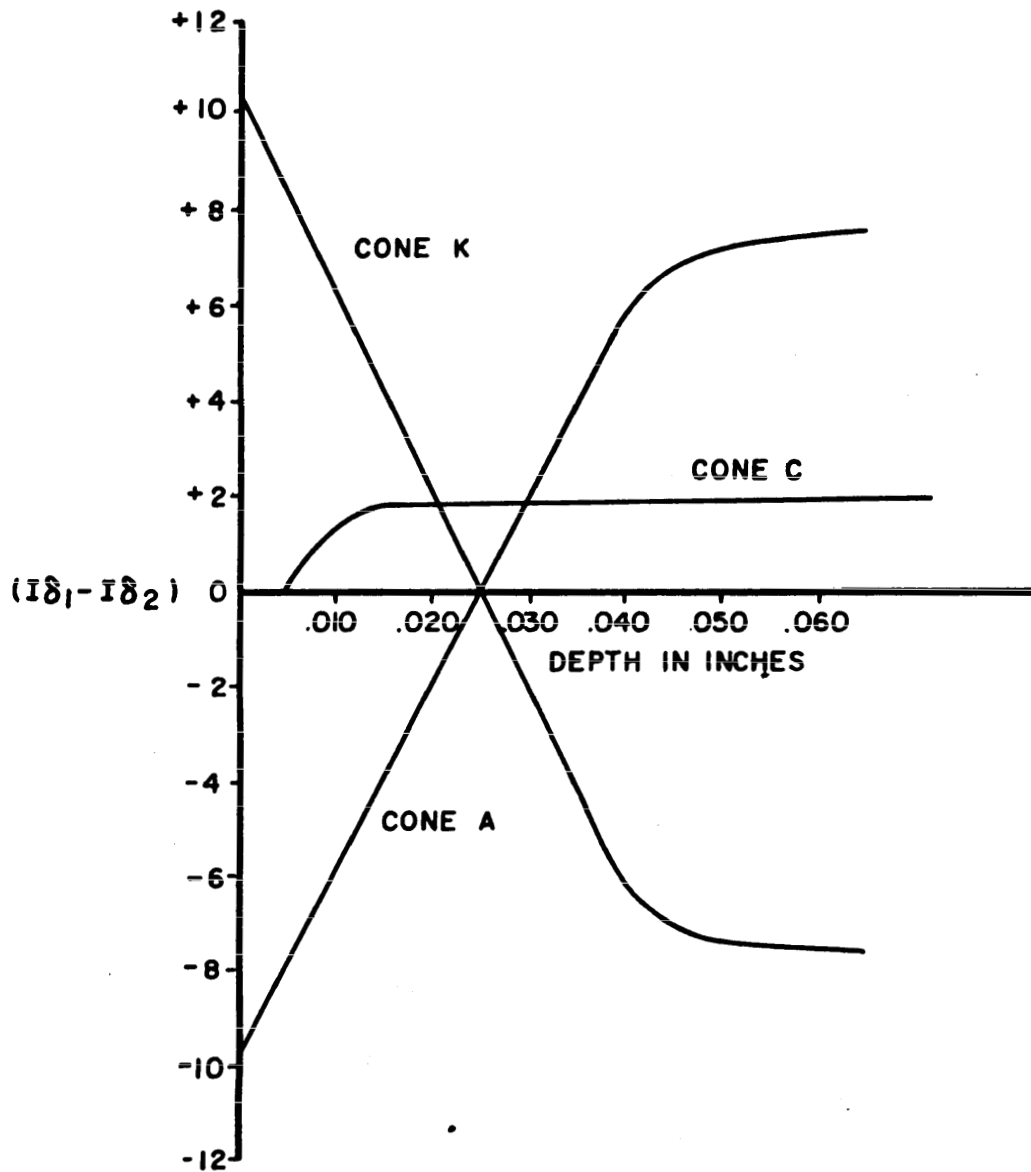
FIG. 22—DIFFERENCE IN INTENSITY MAXIMA FROM THE
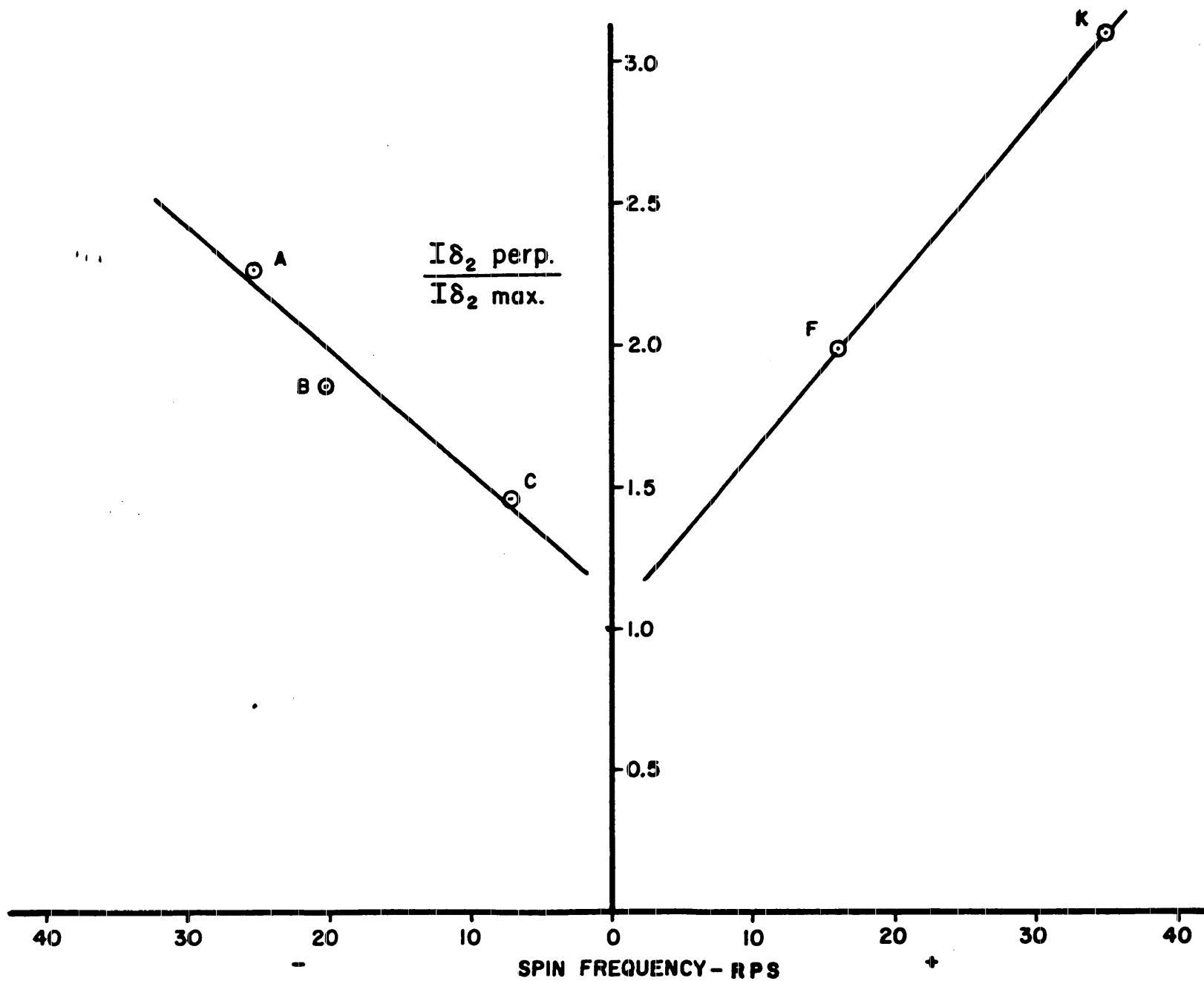SURFACE TO THE INTERIOR OF A CONE WALL

$$\frac{I\delta_2\ \text{perp.}}{I\delta_2\ \text{max.}}$$

SPIN FREQUENCY - RPS

FIG. 23 INTENSITY RATIO VS. SPIN COMPENSATION FREQUENCY
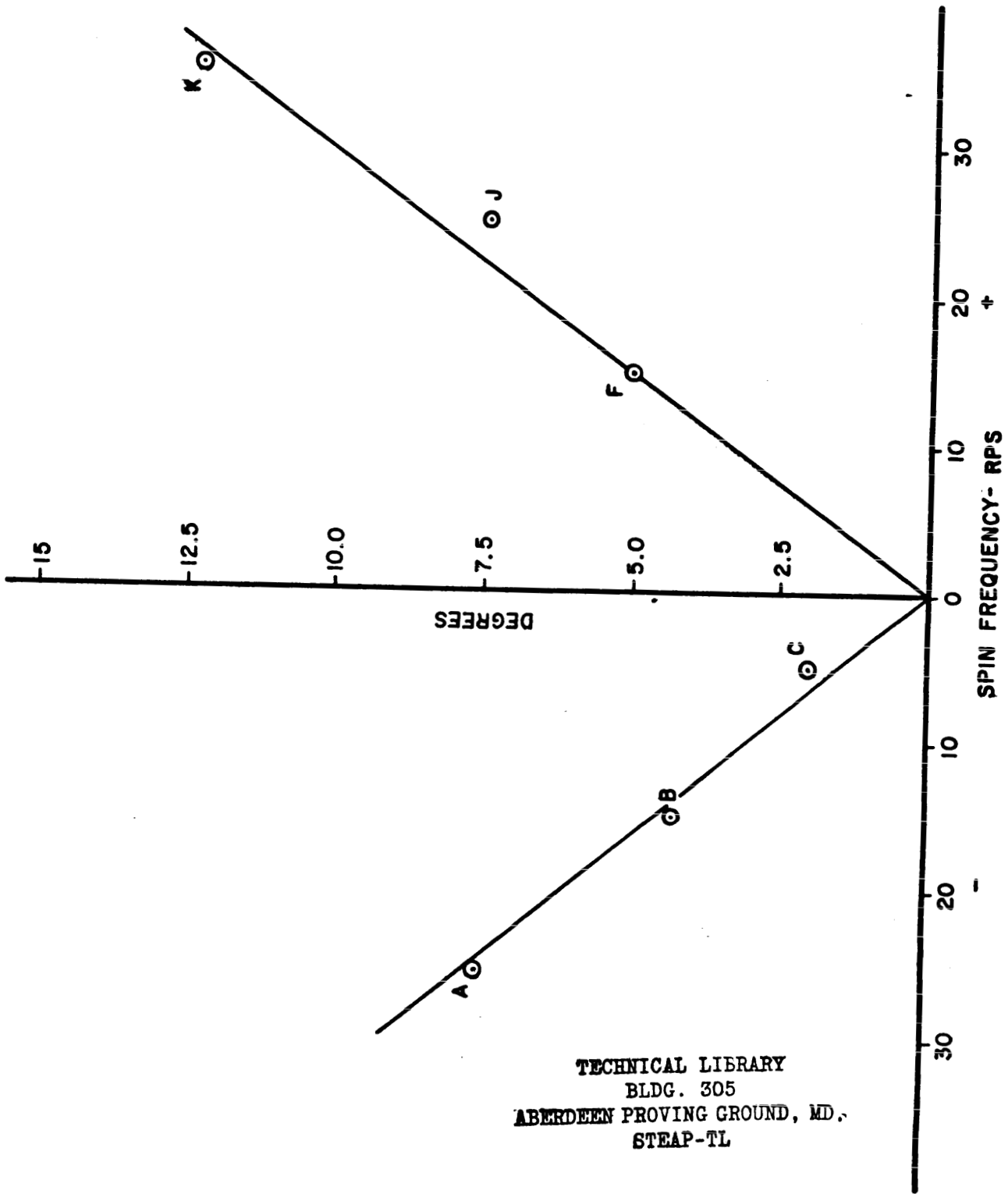
FIG. 24 ANGLE AT WHICH $I\delta_1 = I\delta_2$ VS. SPIN COMPENSATION FREQUENCY

the spin compensation frequency. Figures 23 and 24 show linear relationships of intensity data with spin compensation frequency for the $\{110\}$ plane, within the limit of accuracy of the measurements.

Table IX

Data on the Variation of Intensity Ratios for Different Cone Lots and Different Depths in the Cone Wall

Cone Lot	$I\delta_1\perp/I\delta_1{}_{max}$	$I\delta_2\perp/I\delta_2{}_{max}$	Depth from the Outer Surface
A	2.0	2.75	0.004"
A	2.25	1.80	0.075"
A	2.30	1.89	0.085"
A	2.29	1.75	0.090"
B	1.97	1.72	0.046"
C	1.50	1.39	0.040"
F	2.12	2.39	0.038"
K.	3.27	2.67	0.005"
K	2.33	2.85	0.065"

b. Conclusions from the data.

The following conclusions may be drawn from the data reported above:

(1) The spin-compensation frequency of rotary extruded liners is a function of the concentration of $\{110\}$ planes oriented at a given angle to the surface. Stated another way, as the spin-compensation frequency increases, the difference in intensity of the two maxima found on the diffraction ring increases, indicating the dependence of spin compensation on the grouping of a given plane in one position.

(2) The metal flow in the liner during the forming process is opposite and unequal at the outside and inside surfaces of the liner. The difference in flow between the two surfaces causes a difference in orientation of the intensity maxima from the inside to the outside surfaces.

(3) Since the ratio ($I\delta_1/I\delta$ max), and the angle at which $I\delta_1 = I\delta_2$ vary linearly with spin frequency, it would appear that the more nearly the $\{110\}$ planes lie in the plane of the surface, and the heavier the concentration of planes at a given angle near the surface, the higher the spin frequency.

4. <u>Pole Figure Studies</u>. By rotating the specimen in 5 degree steps above and below normal, and to the left and right of normal, as reported in this Section, Part 2-d, the variation in the concentration of $\{110\}$ planes around a given point is obtained. Due to the limitations imposed on the system by the specimen shape, rotations above 50 degrees from normal are not meaningful. By plotting the concentration of the poles of the $\{110\}$ planes on a stereographic net, where the plane of the net represents the surface of the specimen, a picture is built up of the angular relationships between the $\{110\}$ planes (or poles) and the specimen surface. This has been done for Cone Lots A and K at points 0.010" and 0.085" below the outer surface of the cone, and the results may be seen in Figure 25 a, b, c, and d.

These figures may be read as follows: The circle represents the plane of the specimen and the X-ray beam is striking the specimen perpendicular to this surface. From the center of the projection to an edge represents 90° of arc. The dashed circle on the projections represents the basic diffraction ring of the $\{110\}$ planes when the X-ray beam is perpendicular to the specimen.

The heavy cross-hatched areas represent the highest concentrations of poles of $\{110\}$ planes at the angles to the specimen surface that are measured from the center of the projection to the

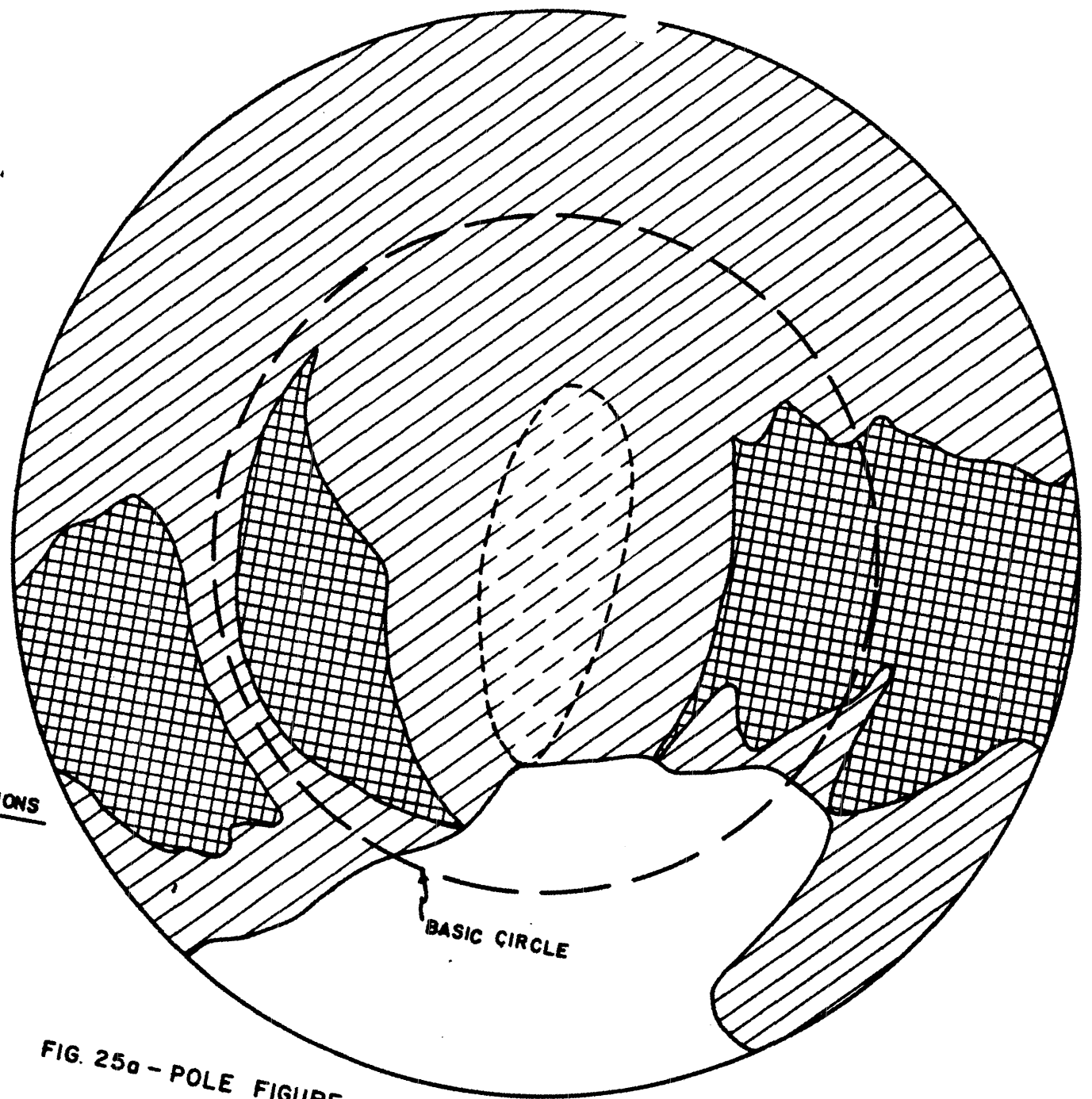LEGEND—$\{1\ 1\ 0\}$
POLE CONCENTRATIONS

▦ HEAVY

▨ MEDIUM

☐ LIGHT

BASIC CIRCLE

FIG. 25a — POLE FIGURE STUDY OF CONE FROM LOT A AT Q10"

99

BASE CIRCLE
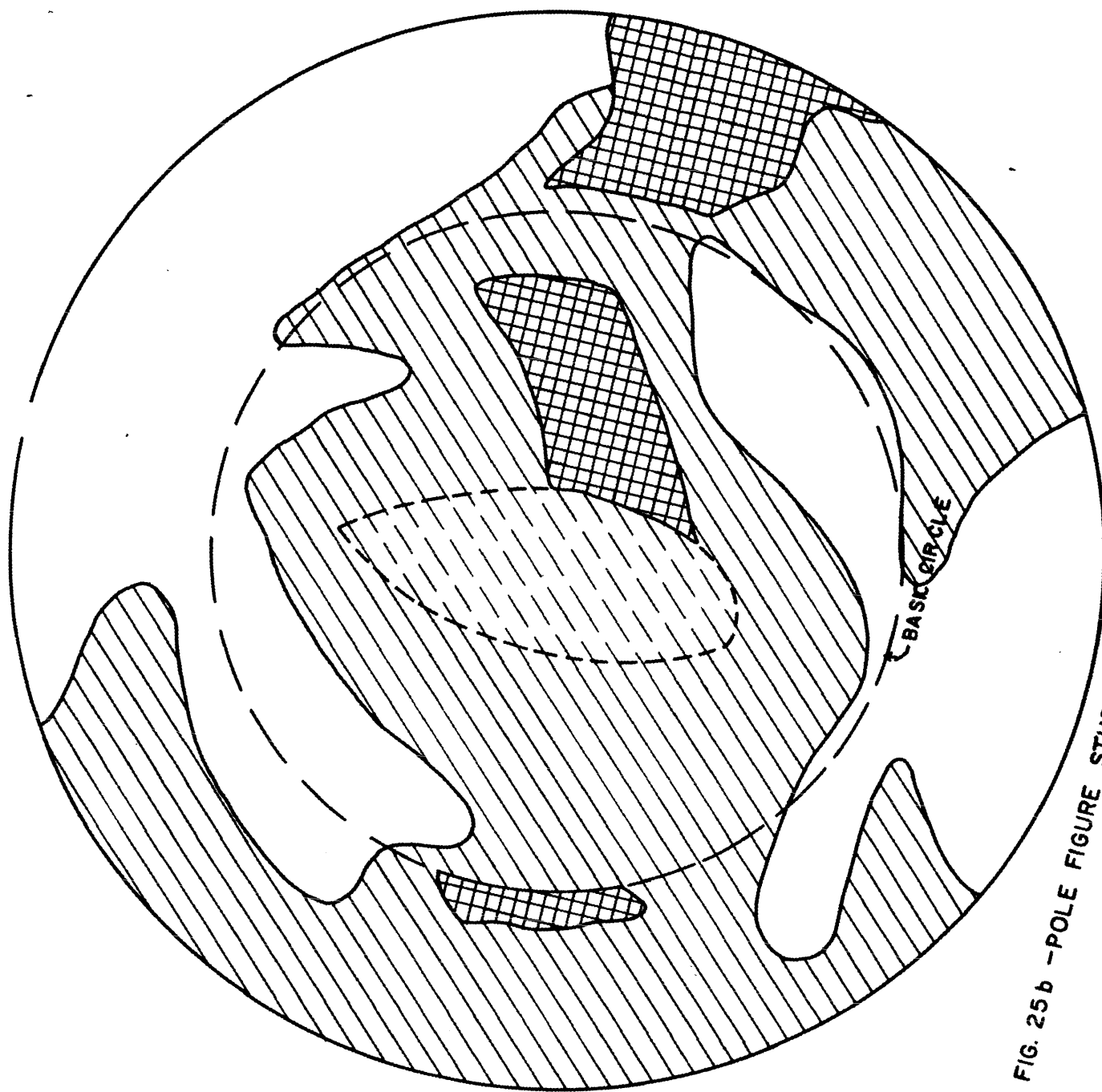
FIG. 25 b — POLE FIGURE STUDY OF CONE FROM LOT K AT Q10"

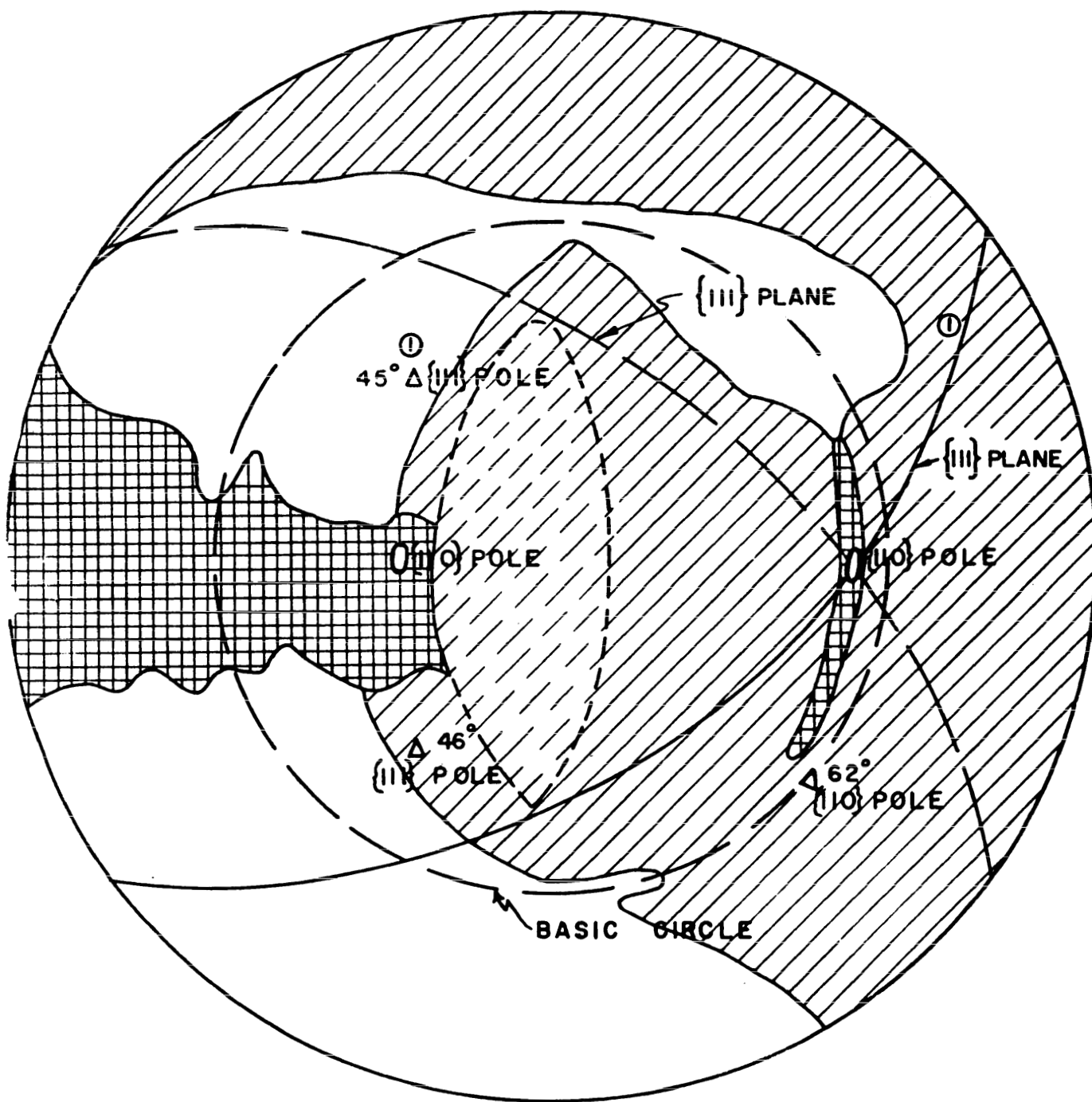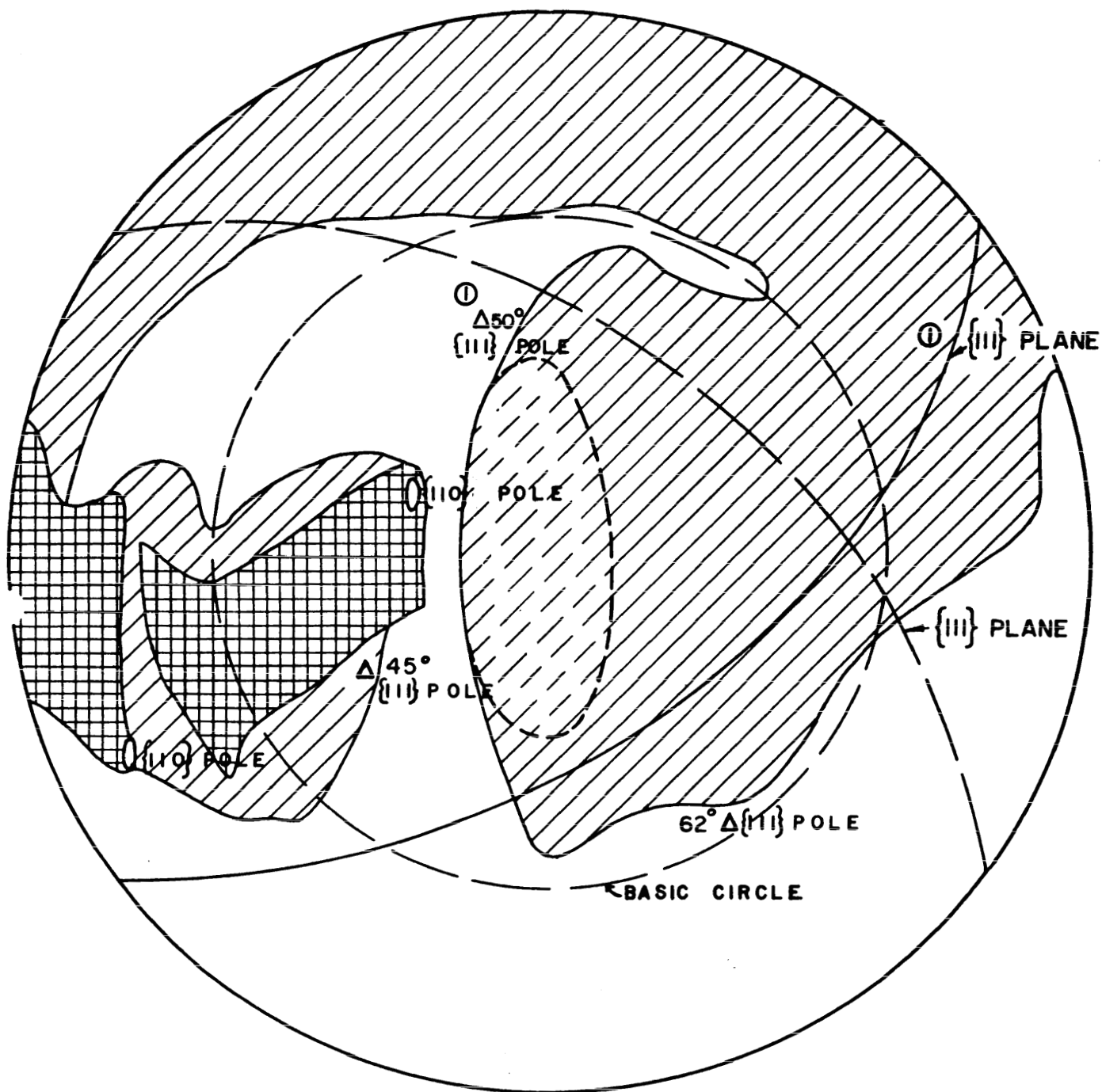FIG. 25 c — POLE FIGURE STUDY OF CONE FROM LOT A AT O85"

FIG. 25d—POLE FIGURE STUDY OF CONE FROM LOT K AT 0.85"

cross-hatched area, using a stereographic net. The areas on the projection with parallel lines through them indicate pole concentrations less than half of that found in the heavily hatched areas. Unmarked regions represent areas where concentrations of $\{110\}$ poles are practically zero.

It is interesting to note the lack of symmetry in these figures. Normal $\{110\}$ pole figures of cold rolled copper would show a symmetrical distribution of heavy and light concentrations of $\{110\}$ poles to the specimen surface, largely due to the fact that more than one slip system operates in metal deformation. Under the conditions of deformation observed here, restrictions in the deformation mode cause concentrations of poles in specific sections without regard to symmetry relationships. The center regions of the pole figures are not filled in with experimental data (indicated by the dashed lines) but are assumed to follow the data near the center.

Poles have been placed on the Figures 25, c and d, to conform with relationships between planes in a single crystal, the single crystal plot being an _ideal_ pole figure since all of the poles of the different planes are concentrated at specific points. In addition, the ideal $\{111\}$ pole relationships have been superimposed on the figures, and are represented by the triangles. Since the $(111)'$ plane is the slip plane in the metal under normal loading, it has been assumed that the (111) plane is still the slip plane under detonation loading.

In the case of cone Lot A, it can be seen in Figure 25c that two $\{111\}$ poles occur at 45° and 46° to the surface, but in Cone Lot K, Figure 25d, only one pole is found to be 45° to the surface, while the other $\{111\}$ poles are at 50° and 62° respectively. These results may be interpreted as follows:

The $\{111\}$ pole at 45 degrees to the surface, which is the pole of a plane $(90-45) = 45^\circ$ from the surface, offers an easy path for collapse of the liner under the detonation loading, providing

70

the path necessary to create a tangential collapse component as discussed previously in the Theory Section, II-c. In the case of Cone A, however, there are two $\{111\}$ poles lying at 45 and 46 degrees to the surface, and consequently two $\{111\}$ planes cut the surface at an angle $(90 - \chi$ of the pole), or $45°$ and $44°$ respectively. It may be argued that the detonation wave moving down the liner surface observes one of the $\{111\}$ planes at the proper angle and collapse starts down that plane. But the other plane at $44°$ feels the effect of the pressure on the surface and some flow will start down it. These two components of flow are cancelling, to a degree, reducing the overall effectiveness of the preferred collapse process. Any orientation that allows one plane to carry most of the collapse process gives more spin compensation, and cone Lot K has only one plane at 45 degrees, while the other plane is located at 40 degrees to the surface.

This is an oversimplification of the problem. The qualitative nature of the data restricts complete analysis as to the proper slip direction in the slip plane. At the present time, however, that is not necessary if it can be demonstrated that a metal will collapse crystallographically, or deform along crystallographic planes under detonation loading. This has been attempted, and results from one such experiment are reported in the next section.

E. Determination of Deformation Mode of a Copper Single Crystal Under Explosive Impulse

   1. Experimental Procedure. If the implications in the above analysis are correct, it should be possible to deform single crystals with explosives and observe the deformation process taking place along crystallographic directions on certain crystal planes. To determine whether or not this is true, a simple experiment in impulsive loading of a single crystal was undertaken, the results of which are described here.

Referring to Figure 26, a single crystal cylinder of copper, 2.8" outside diamter and 1 1/4" long, with an inside diameter of 0.75", was loaded with an explosive charge in the center, and detonated from one end. Figure 27 shows a recovered section of the cylinder after the detonation. The following data were recorded in the experiment:

a. Framing camera pictures were taken observing the end of the cylinder as it deformed. The framing speed was approximately 10^5 frames a second.

b. Back-reflection Laue X-ray pictures were made of the specimen, before and after deformation, at the same point on the crystal.

c. Measurements were made on the change in shape and the change in orientation of the crystal due to the deformation.

2. Results. Figure 28 is a stereographic plot of the poles of the $\{100\}$, $\{110\}$, and $\{111\}$ planes in the crystal before and after deformation, as determined by X-ray analysis. The end of the single crystal cylinder lies in the plane of the paper, the specimen axis lying directly in the center of the plot. The poles would cut the surface as indicated. It may be seen that a rotation of the poles about the specimen axis has occurred during the deformation process. This may be interpreted in another manner; the specimen axis has rotated its position with respect to the poles of the planes in the single crystal. This is what would be expected if the metal failed along crystallographic planes. Figure 29 is a plot of the specimen axis in a standard cubic stereographic projection triangle, before and after deformation. The movement of the specimen axis is similar to that movement which is expected under normal loading conditions.

Matching fractured surfaces in the deformed crystal, it can be seen that metal flow has taken place in such a manner as to "square up" the cylinder, as seen in Figure 27. There are two stress fields
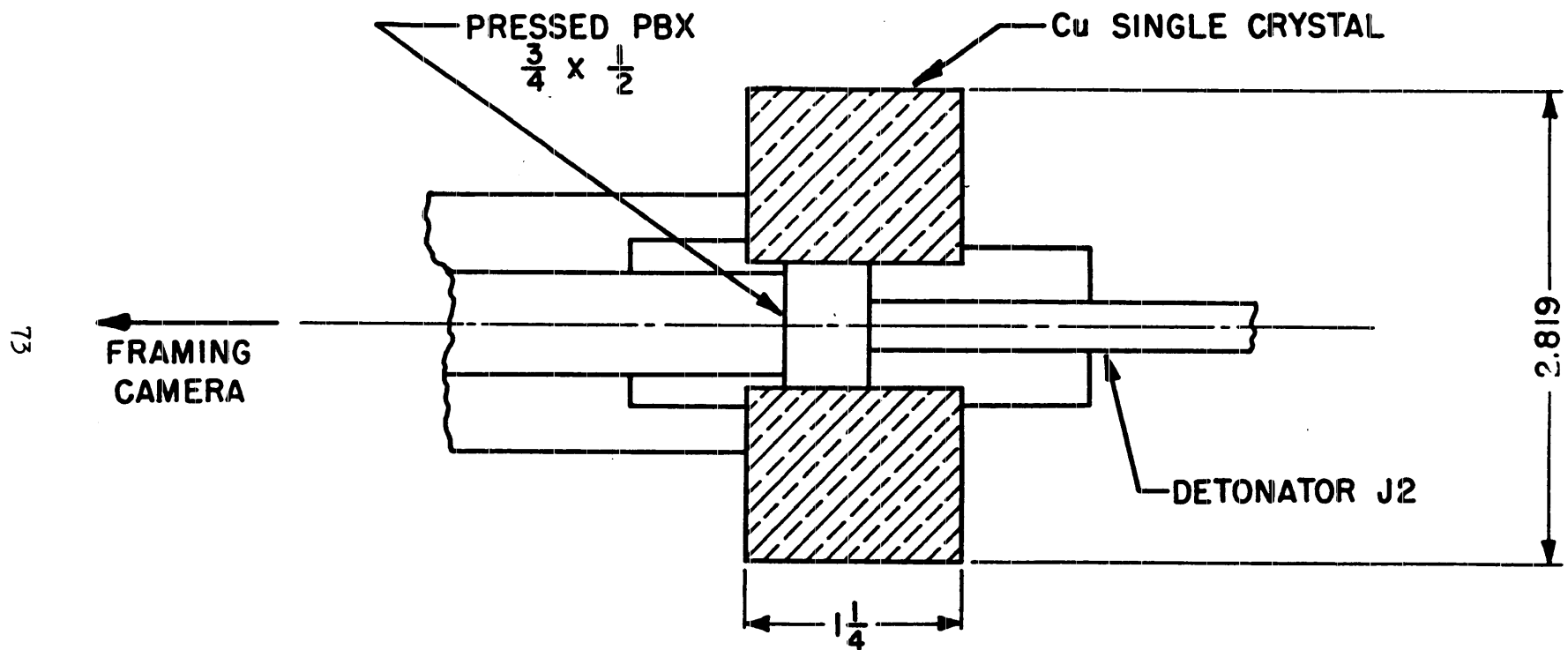
FIG. 26   CROSS SECTION OF SINGLE CRYSTAL CYLINDER

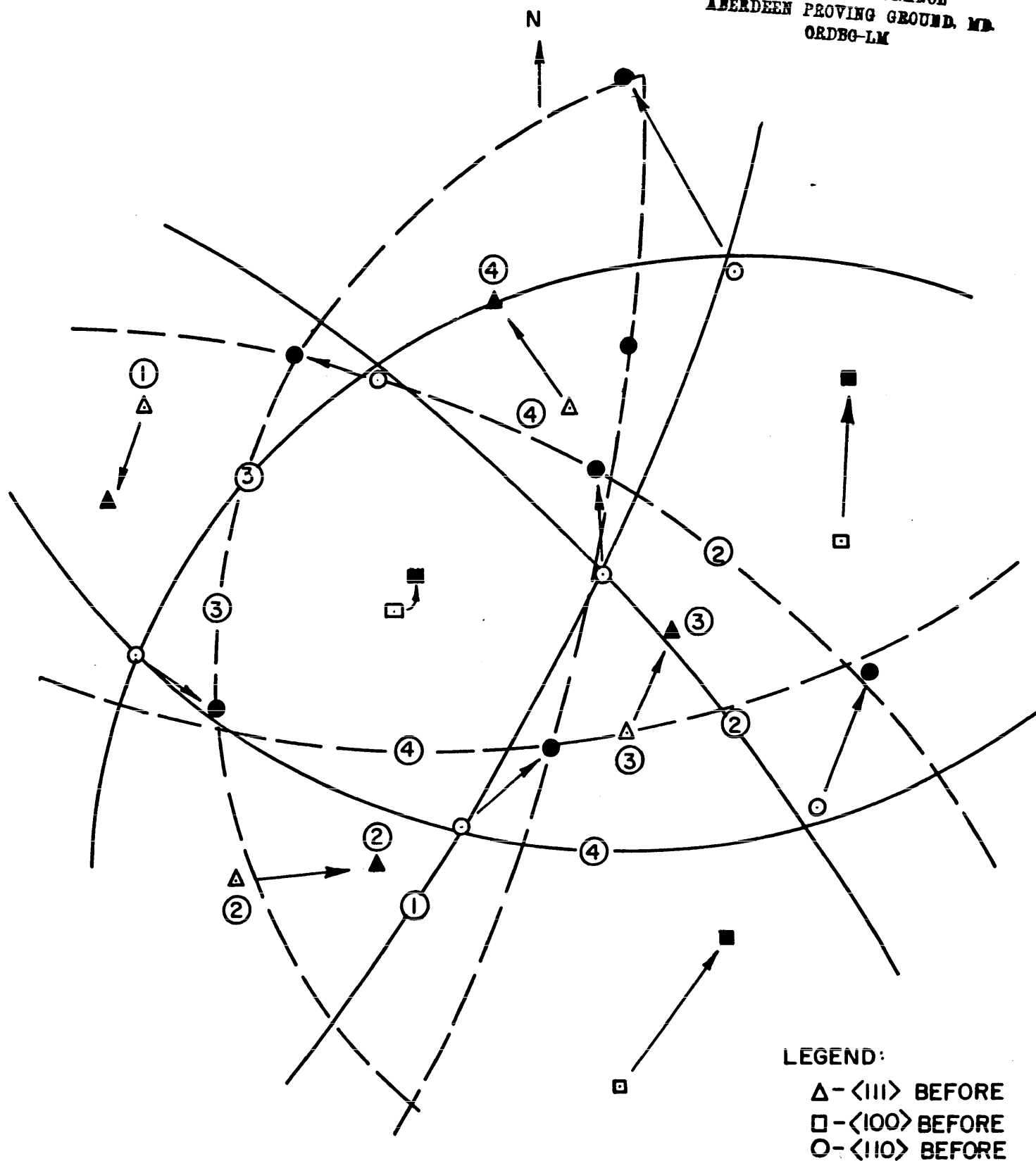FIG. 27 RECOVERED SECTION OF THE SINGLE CRYSTAL

N

FIG. 28 — STEREOGRAPHIC PLOT OF ⟨I00⟩ ⟨II0⟩ AND ⟨III⟩ TYPE
POLES, BEFORE AND AFTER DEFORMATION
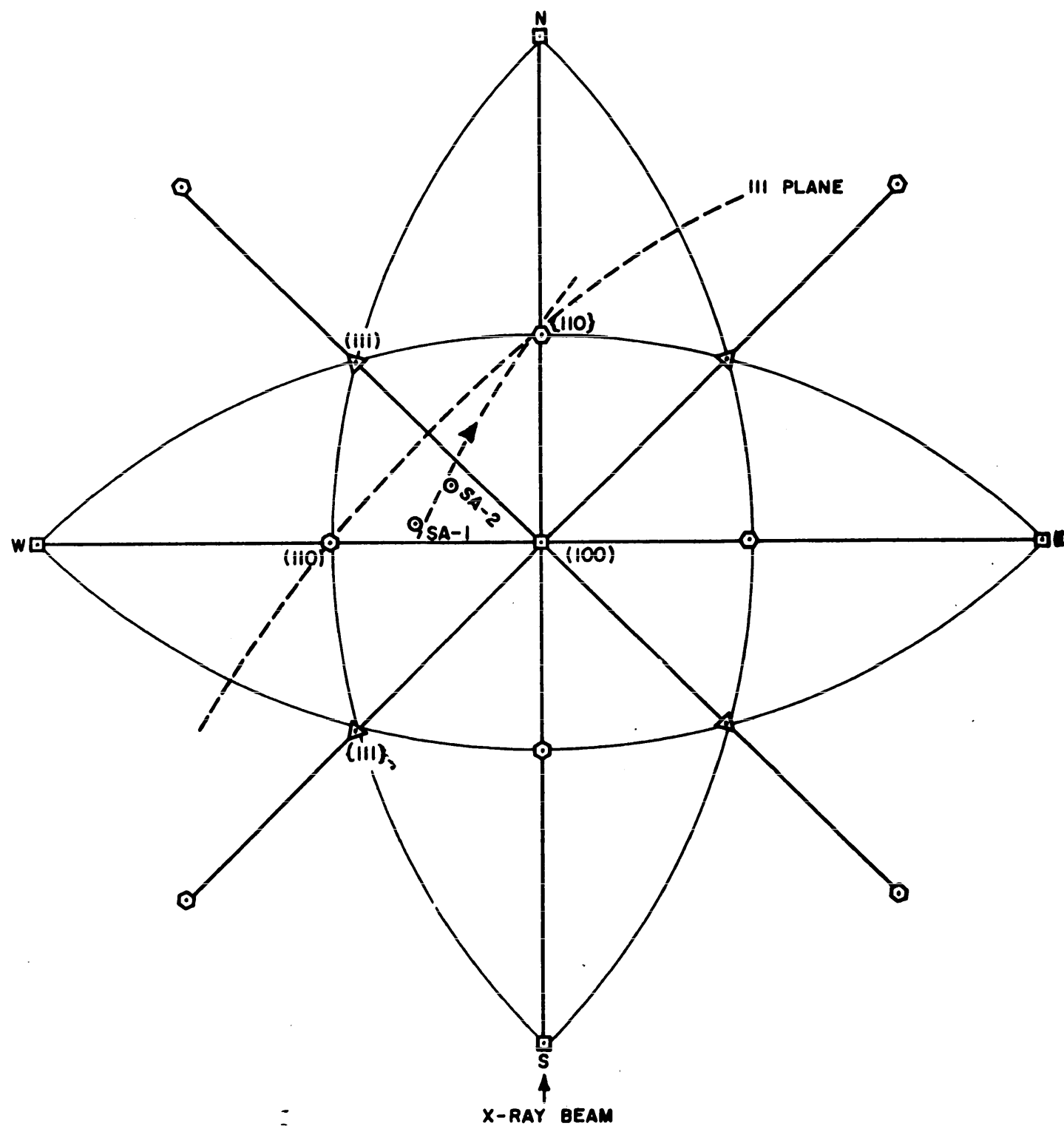
FIG. 29   PLOT OF THE SPECIMEN AXIS IN A STANDARD
TRIANGLE BEFORE AND AFTER DEFORMATION

of importance in the deformation: (1) tensile stresses developed through release waves, resolved in a direction parallel to the cylinder axis; and (2) tangential tensile forces in the cylinder wall due to the internal pressure. These produce crystallographic flow and fracture.

Figure 30, a and b, represents the cylinder end before and after the deformation. Using the stereographic plots, the intersections of the $\{111\}$ planes and the cylinder surface were placed in position on the cylinder end. Flow along these $\{111\}$ planes under the combined stresses would reduce the cylinder walls at the proper places, building them up at the points noted in the pictures, and tending to form a square.

3. <u>Conclusions</u>. While the above discussion is an over-simplication of the analysis involved, the following conclusions can be deduced (applying to the given set of experimental conditions used):

a. Crystallographic flow begins early in the deformation process.

b. Flow occurs predominantly along the $\{111\}$ plane in the $[110]$ direction with consequent rotation of the specimen axis.
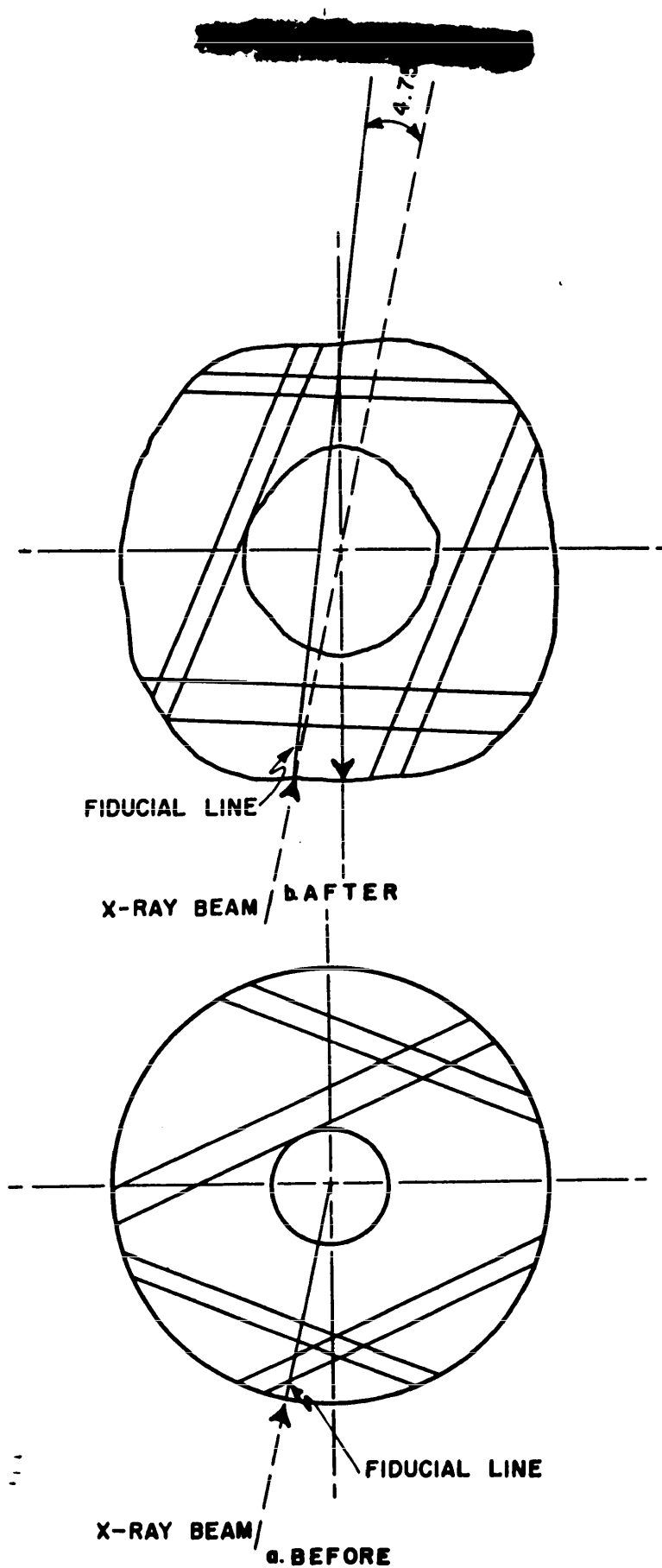
FIDUCIAL LINE

X-RAY BEAM / b.AFTER

FIDUCIAL LINE

X-RAY BEAM /

a. BEFORE

FIG. 30 – SINGLE CRYSTAL {III} PLANES BEFORE AND
AFTER FIRING.

78

The causative relationship between spin compensation in rotary-extruded liners and the asymmetric orientation of the grain structure in the metal is evident from the experimental results. It is also clear that the mechanism described for the deformation of the liner metal under the explosive impulse will result in a tangential component of the collapse velocity and consequently in a tendency for spin compensation. The model presented, however, does not explain in what manner the angular momentum of the liner is conserved during the process.

A somewhat different approach to the model of the phenomenon is perhaps more convenient for the purpose of considering conservation of angular momentum. The preferred directions of deformation resulting from the grain orientation can be described in an entirely equivalent fashion as an orientation of the shock pulse traversing the oriented grains. If the transfer of energy takes place more rapidly along close packed atomic planes than along those in which packing is less dense, a highly localized orientation of the shock wave takes place which will be governed by the degree and direction of the grain orientation. Furthermore, the orientation of the initial compressive shock traversing the metal will be preserved upon reflection from the free inner surfaces of the liner in the reflected tension wave.

A net change in angular momentum of the liner material cannot be effected during the time required for the initial compression wave to traverse the liner from outer to inner surface, since there is no other portion of the system to which momentum can be transferred. On the other hand, when the reflected tension wave arrives at the outer surface of the liner, having, at least in a highly localized sense, a tangential component of velocity, a transfer of angular momentum to the surrounding gaseous products of detonation can be expected. Furthermore, the direction of the angular momentum transfer to the gases will be opposite to the change in angular momentum of the liner metal. In this

way, a net change in the angular momentum of the metal liner could be effected and, consequently, the angular momentum of the system as a whole conserved.

A similar mechanism of transfer of angular momentum has been proposed for fluted liners having flutes on the inner surface only.[25] As in the case of the rotary extruded liner, there is no apparent mechanism by which angular momentum can be transferred prior to the arrival of the reflected tension wave at the outer surface of the liner. In the case of the fluted liner, the orientation of the reflected tension wave is produced by the asymmetric fluted geometry of the inner surface. As in the case of the rotary-extruded liners, liners having flutes on the inner surface only have been observed to produce only relatively small spin-compensation frequency. This observation is entirely reasonable in view of the attenuation of the product gases during the time required for the initial compressive shock and the reflected tension wave to traverse the wall of the liner. Under these conditions, the surrounding gases will have lower density than immediately after the passage of the detonation wave and would presumably be capable of absorbing less angular momentum. In addition, the attenuation of the shock wave while traversing twice the thickness of the liner would tend to limit the magnitude of the compensation frequency attainable.

In the case of liners having flutes on the external surface, the transfer of angular momentum to the product gases can take place immediately upon arrival of the detonation wave at a cross-section of the liner, since the orientation of the shock reflected into the product gases is effected by the external geometry of the liner. Consequently, it would be expected, as observed, that liners having asymmetric external geometries would produce higher compensation frequencies than either liners having only internal flutes or rotary-extruded liners.

Experimental support for the mechanism proposed is obtained from two short experiments in which the velocity of propagation of deformation

waves in single crystals have been measured. Unpublished results by
Messrs. Hauver and Moss, of the BRL, have noted the following results
for the deformation wave velocity:

    (1) Single Crystalline Copper Specimen.

        (100) type plane perpendicular to the deformation wave:
$$V = 4.65 \text{ mm}/\mu s$$

    (2) Single Crystalline Copper Specimen.

        (211) type plane perpendicular to the deformation wave:
$$V = 4.68 \text{ mm}/\mu s$$

    (3) Polycrystalline Copper Specimens: $V = 4.50 \text{ mm}/\mu s$

While the differences in propagation velocities observed are small,
the effect being explained is also small, so that the correlation is not
unreasonable.

The second source of support is a series of experiments conducted
by Mr. J. Simon of BRL on liners made by rotary extrusion and having
flutes on the interior surface.[26] In this experiment, it was observed
that the net spin compensation frequency of the liner was the sum of
the frequencies to be expected from the rotary extrusion process alone
and from the flutes alone, indicating that the total tangential com-
ponent of the re-oriented shock wave was the resultant of the components
arising from the two separate mechanisms.

In conclusion, it is conceivably possible to increase the spin
compensation rate of rotary extruded liners if a heavier concentration
of planes can be formed at the proper angle to the cone surface. By
proper processing of the blank material used in forming the cones, a
heavier preferred orientation may be expected in the finished cone.

However, attempts to do this will be delayed until experimental evidence is obtained concerning the practical limitations imposed on the system by the difference in shock velocities between crystal planes and the polycrystalline metal.

COY M. GLASS

M. K. GAINER

G. L. MOSS

BIBLIOGRAPHY

1. Birkhoff, G., MacDougall, D.P., Pugh, E. M. and Taylor, G. "Explosives with Lined Cavities", Journal of Applied Physics, Volume 19, Number 6, June 1948 (563-582).

2. Pugh, E. M., Eichelberger, R. J., Rostoker, N. "Theory of Jet Formation by Charges with Lined Conical Cavities", Journal of Applied Physics, Volume 23, Number 5, May 1952 (532-36).

3. Eichelberger, R. J. and Pugh, E. M. "Experimental Verification of the Theory of Jet Formation", Journal of Applied Physics, Volume 23, No. 5, May 1952 (537-542).

4. Eichelberger, R. J. "Re-examination of the Non-steady Theory of Jet Formation by Lined Cavity Charges", Journal of Applied Physics, Volume 26, Number 4, April 1955 (398-402).

5. Eichelberger, R. J. "Spin Compensation", Critical Review of Shaped Charge Information, BRL Report No. 905, May 1954 (215-).

6. Litchfield, E. L. and Eichelberger, R. J. "Spin Compensation by Back to Back Flutes", The Ordnance Corps Shaped Charge Research Report, No. 2-55, April 1955.

7. Supplement to the Sixth Progress Report of the Firestone Tire and Rubber Company on Contract DA 1-53-019-501-ORD 16, "Design and Development of Cartridge HEAT, T300 for 90 MM Gun, T119, October 1953, Akron, Ohio, and Forty-first Progress Report of the Firestone Tire and Rubber Company, on BAT Project, Contracts DA 33-019-ORD 33 and DA 33-019-ORD 1202, December 1953, Akron, Ohio.

8. Kronman, S., Simon, J., Rayfield, F. and Zernow, L. "A Triple-Flash Field Radiographic System for Studying Jets from Large Shaped Charges", BRL Memorandum Report No. 659, March 1953.

9. Simon, J. "Flash Radiographic Study of Anomalous Jets from 90 MM Liners Manufactured by Rotary Extrusion", BRL Memorandum Report Number 907, July 1955.

10. Simon, J. "Flash Radiographic Study of Jets from Rotary Extruded Shaped Charge Liners", The Ordnance Corps Shaped Charge Report, Number 2-56, April 1956.

11. Simon, J. "Flash Radiographic Study of Spin Compensation with 105 MM Fluted Liners (II)", The Ordnance Corps Shaped Charge Research Report, Number 4-55, October 1955.

12. Kessler, S. W., Simon, J. and Cox, J. J. "Rotary Extrusion of Shaped Charge Liners", The Ordnance Corps Shaped Charge Research Report, Number 1-56, January 1956.

13. Simon, J. and Martin, T. H. "Spin Compensation of Shaped Charge Liners Manufactured by the Rotary Extrusion Process", BRL Memorandum Report Number 1181, December 1958.

14. Zernow, L. and Simon, J. "Flash Radiographic Study of Spin Compensation in Shear Formed Liners (ITE)", The Ordnance Corps Shaped Charge Report, Volume 1, Number 1, July 1954.

15. Simon, J. and Zernow, L. "Metallurgical Spin Compensation in Smooth Electroformed Liners", The Ordnance Corps Shaped Charge Research Report, Volume 1, Number 1, July 1954.

16. Simon, J. "Flash Radiographs of Jets from 105 MM Electroformed Cobalt Liners", The Ordnance Corps Shaped Charge Research Report, Number 1-56, January 1956.

17. Simon, J. "Rotary Extruded Shaped Charge Liners of Brass Alloys and Armco Iron", The Ordnance Corps Shaped Charge Research Report, Number 1-56, January 1956.

18. Simon, J. and Martin, T. H. "Flash Radiographic Observations on Lead Antimony Rotary Extruded Liners", The Ordnance Corps Shaped Charge Research Report, Number 1-57, January 1957.

19. Simon, J. "Flash Radiographic Study of Jets from Rotary Extruded Shaped Charge Liners", The Ordnance Corps Shaped Charge Research Report, Number 2-56, April 1956.

20. Watson, J. F. "Preferred Orientation in Shear Formed Liners (ITE)", The Ordnance Corps Shaped Charge Research Report, Number 2-55, April 1955.

21. Koch, R., Simon, J. and Zernow, L. "Flash Radiographic Study of Jets from Single Crystal Aluminum Liners", The Ordnance Corps Shaped Charge Research Report, Number 3-55, July 1955.

22. Koch, R., Zernow, L. and Simon, J. "Initial Study of Jets from Single Crystal Copper Cones with the (100) Direction Near the Cone Axis", The Ordnance Corps Shaped Charge Research Report, Volume 1, Number 2, October 1954.

23. Zernow, L., Regan, J. and Simon, J. "Jets from Liners Manufactured from Twisted Copper Bars", The Ordnance Corps Shaped Charge Research Report, Number 1-56, January 1956.

24. Carrier, G. F. and Prager, W. "Influence of Residual Stresses on Liner Performances", Technical Report Number 1, Contract DA-3426/1, Brown University, Providence, Rhode Island, 1955.

25. Dreesen, J. A. and Eichelberger, R. J. "Spin Compensation: Theoretical Treatment of Liners Fluted Inside Only", Final Report on Contract DA 503-04-009, Fundamentals of Shaped Charges, Carnegie Institute of Technology, Pittsburgh, Pennsylvania, October 31, 1954.

26. Simon, J. "Flash Radiographic Studies and Penetration Performance of Jets from Special Rotary Extruded Shaped Charge Liners", Transactions of the Symposium on Shaped Charges, BRL, APG, May 22-24, 1956.

DISTRIBUTION LIST

No. of Copies	Organization	No. of Copies	Organization
1	Chief of Ordnance Department of the Army Washington 25, D. C. Attn: ORDTB - Bal Sec (1 cy) ORDIM - Mr. A. Wilkinson	1	Commander U. S. Naval Ordnance Test Station China Lake, California Attn: Technical Library
1	Commanding Officer Diamond Ordnance Fuze Laboratories Washington 25, D. C. Attn: ORDTL - 012	1	Commander U. S. Naval Weapons Laboratory Dahlgren, Virginia
1	Commanding Officer Diamond Ordnance Fuze Laboratories Washington 25, D. C.	3	Commander Air Proving Ground Center Eglin Air Force Base, Florida Attn: PGTRI PGW PGR
10	Director Armed Services Technical Information Agency Arlington Hall Station Arlington 12, Virginia Attn: TIPCR	1	Commander Air Research & Development Command Andrews Air Force Base Washington 25, D. C. Attn: RDTWMB
10	British Joint Services Mission 1800 K Street, N. W. Washington 6, D. C. Attn: Reports Officer	1	U. S. Atomic Energy Commission Los Alamos Scientific Laboratory P. O. Box 1663 Los Alamos, New Mexico
4	Canadian Army Staff 2450 Massachusetts Ave., N. W. Washington 8, D. C.	1	U. S. Atomic Energy Commission Washington 25, D. C. Attn: Technical Reports Library Mrs. J. O'Leary for Division of Military Application
3	Chief, Bureau of Ordnance Department of the Navy Washington 25, D. C. Attn: ReO	1	U. S. Bureau of Mines Department of the Interior 4800 Forbes Street Pittsburgh 13, Pennsylvania Attn: Chief, Explosive & Physical Sciences Division
2	Commander Naval Ordnance Laboratory White Oak Silver Spring 19, Maryland		

DISTRIBUTION LIST

No. of Copies	Organization	No. of Copies	Organization
1	Library of Congress Technical Information Div. Reference Department Washington 25, D. C. Attn: Bibliography Section	1	Commanding Officer Detroit Arsenal 28251 Van Dyke Avenue Centerline, Michigan
1	Commanding General Continental Army Command Fort Monroe, Virginia	1	Commanding General Frankford Arsenal Bridge & Tacony Streets Philadelphia 37, Pa.
1	President U. S. Army Armor Board Fort Knox, Kentucky	1	Commanding Officer Office of Ordnance Research Box CM, Duke Station Durham, North Carolina
1	President U. S. Army Infantry Board Fort Benning, Georgia	1	Commanding Officer Ordnance Ammunition Command Joliet, Illinois Attn: ORDLY-AR-V 　　　 ORDLY-AR-AR
1	Commanding Officer Rock Island Arsenal Rock Island, Illinois	1	Applied Physics Laboratory 8621 Georgia Avenue Silver Spring, Maryland
1	Commanding Officer Ordnance Weapons Command Rock Island, Illinois Attn: Research Branch		THRU: Naval Inspector of 　　　　 Ordnance 　　　　 Applied Physics Lab. 　　　　 8621 Georgia Avenue 　　　　 Silver Spring, Maryland
3	Commanding Officer Picatinny Arsenal Dover, New Jersey Attn: Feltman Research & 　　　　 Engineering Lab.	2	Aerojet-General Corporation 6352 North Irwindale Road Azusa, California Of Interest to:
1	Commander Army Rocket & Guided Missile 　 Agency Redstone Arsenal, Alabama Attn: Technical Library 　　　　 ORDXR-OTL		Mr. Guy C. Throner, Chief 　　　 Explosive Ordnance Station 　　　 Dr. Louis Zernow THRU: Bureau of Aeronautics Rep. 　　　　 Aerojet-General Corp. 　　　　 6352 North Irwindale Ave. 　　　　 Azusa, California
1	Commanding Officer Watertown Arsenal Watertown 72, Mass. Attn: W. A. Laboratory		

DISTRIBUTION LIST

No. of Copies	Organization
1	Carnegie Institute of Technology Department of Physics Pittsburgh 13, Pa. Attn: Dr. Emerson M. Pugh THRU: Commanding Officer Philadelphia Ordnance District 1500 Chestnut St. Philadelphia 2, Pa.
1	Firestone Tire & Rubber Co. Akron 17, Ohio Attn: Librarian Mr. C. M. Cox Defense Research Div. THRU: Commanding Officer Cleveland Ordnance District 1367 East Sixth Street Cleveland 14, Ohio
1	Army Research Office Arlington Hall Station Arlington, Virginia
1	Director Defense Res & Engr (OSD) Director/Ordnance Washington 25, D. C.

AD _____ Accession No. _____

Ballistic Research Laboratories, APG
EFFECTS OF ANISOTROPIES IN ROTARY EXTRUDED LINERS
C. M. Glass, M. K. Gainer and G. L. Moss

BRL Report No. 1084 November 1959

DA Proj No. 503-04-009, ORD Proj No. TB3-0134
Report

Performance
Shaped charges - Design

Conical shaped charge liners manufactured by the rotary extrusion process exhibit a characteristic "spin compensation" not found in an ordinary liner. It has been determined that this ability to counteract degradation of the jet when the round is being subjected to an external rotation is dependent on the manner in which certain crystal planes are aligned with respect to the surface of the cone. Direct correlation between the preferred orientation of the planes and the spin compensation frequency has been found. In addition, it has been demonstrated that other factors, such as residual stress, grain shape, etc., do not influence the compensation rate.

It is proposed that under detonation loading there exists a component of collapse velocity of the liner wall that is not directed toward the axis of the cone. This tangential component results from the preferred orientation of the crystal planes, and gives an angular velocity to the collapsing cone elements that compensates for the angular velocity due to external rotation of the round. Experimental evidence is offered to show that a metal having a strong preferred orientation will deform anisotropically under detonation loading.